

Byzantine-Robust Federated Learning Using Generative Adversarial Networks

Usama Zafar
Uppsala University
usama.zafar@it.uu.se

André Teixeira
Uppsala University
andre.teixeira@it.uu.se

Salman Toor*
Uppsala University
salman.toor@it.uu.se

Abstract

Federated learning (FL) enables collaborative model training across distributed clients without sharing raw data, but its robustness is threatened by Byzantine behaviors such as data and model poisoning. Existing defenses face fundamental limitations: robust aggregation rules incur error lower bounds that grow with client heterogeneity, while detection-based methods often rely on heuristics (e.g., a fixed number of malicious clients) or require trusted external datasets for validation. We present a defense framework that addresses these challenges by leveraging a conditional generative adversarial network (cGAN) at the server to synthesize representative data for validating client updates. This approach eliminates reliance on external datasets, adapts to diverse attack strategies, and integrates seamlessly into standard FL workflows. Extensive experiments on benchmark datasets demonstrate that our framework accurately distinguishes malicious from benign clients while maintaining overall model accuracy. Beyond Byzantine robustness, we also examine the representativeness of synthesized data, computational costs of cGAN training, and the transparency and scalability of our approach.

1 Introduction

The success of modern machine learning hinges on access to large and diverse datasets. Applications such as personalized healthcare, finance, and recommendation systems benefit from data-rich models, but centralizing sensitive data raises severe privacy and regulatory concerns. High-profile incidents, including the Facebook–Cambridge Analytica scandal [4] and the Equifax breach [9], illustrate the risks of centralized data storage, while privacy regulations such as the GDPR [35] and CCPA [16] impose strict limits on data collection and sharing. These developments have accelerated the adoption of federated learning (FL) [24], which enables multiple organizations or devices to collaboratively train models without exposing raw data. Despite its privacy-preserving promise,

FL is vulnerable to Byzantine failures, where some clients behave arbitrarily due to faults or adversarial manipulation. Among these, model poisoning [6, 13] has emerged as the most damaging threat, enabling adversaries to degrade overall model accuracy and hinder convergence.

Efforts to defend against Byzantine behavior have followed two broad directions. One approach employs Byzantine-robust aggregation rules such as Krum [3], Coordinate-wise Median [38], and Trimmed Mean [38], which reduce the influence of corrupted updates through statistical filtering. While effective in homogeneous settings, these methods face fundamental limitations: their error guarantees scale poorly with the variance of client updates, restricting robustness in heterogeneous FL environments [1, 19]. A second direction leverages detection-based strategies that aim to identify and filter malicious clients [5, 33, 40, 41]. These often depend on heuristics such as assumed Byzantine fractions or external validation datasets—assumptions that are impractical in real deployments and misaligned with FL’s privacy objectives. Moreover, static detection rules are brittle against adaptive adversaries whose strategies evolve during training.

Within this second direction, Zhao *et al.* [41] introduced a GAN-based defense that validates updates using auxiliary data. While generative approaches show promise, reliance on external validation datasets undermines privacy guarantees and limits deployability in federated settings. To overcome this, we propose a filter-based defense that leverages a conditional generative adversarial network (cGAN) trained solely from the global model itself. Our method requires no client-side or auxiliary datasets, thereby avoiding additional privacy leakage. By generating synthetic inputs tailored to the evolving global model, the defense adapts naturally to shifting attack strategies. Further, it integrates seamlessly into standard FL workflows without modifying client procedures, offering a practical path toward robust, privacy-preserving, and deployable defenses.

Research Focus & Contributions. Our study investigates how decision boundaries evolve in federated learning under

*Also CTO at Scaleout Systems.

adversarial influence, and how synthetic data can be leveraged to probe these boundaries for robust and privacy-preserving defense. Unlike natural training data, our GAN-generated samples are not limited to dense data regions but are distributed across the input space to better distinguish benign from malicious updates, without exposing any client data. While GANs themselves are not new, our contribution lies in leveraging their ability to generate boundary-respecting samples that may appear unrealistic to humans but remain meaningful to the model. This perspective allows us to analyze how poisoned updates shift the global decision surface and to design detection mechanisms that are effective and privacy-preserving. We also evaluate its computational cost and illustrate the spread of synthesized data across decision boundaries using a toy example, which demonstrates how our method supports a robust defense (further elaborated in Section 4).

To summarize, this paper makes the following key contributions:

- **First GAN-based defense without external data.** We show that GANs can be trained entirely from the global model itself, enabling the server to generate synthetic data for validating client updates without auxiliary datasets.
- **Decision-boundary informed detection.** By generating samples that respect decision boundaries beyond dense regions, our method provides model-relevant probes that reveal poisoned behavior even if the generated samples are not human-interpretable.
- **Privacy-preserving and adaptive.** The defense detects malicious contributions without accessing client data and without relying on static thresholds or additional hyperparameters, simplifying deployment and improving robustness against diverse attack strategies.
- **Robustness and deployability.** Extensive evaluations across datasets and architectures show that our defense reliably distinguishes malicious from benign clients while maintaining model accuracy, with computational costs analyzed to demonstrate practicality for real-world FL systems.

2 Background and Related Work

2.1 Federated Learning Overview

Federated Learning (FL) [24, 37] is a distributed training paradigm that enables collaborative model training across multiple clients, each holding local datasets, without directly sharing data. This paradigm improves privacy by ensuring that raw data remains on-device, while only model updates are communicated.

Table 1: Summary of notations used throughout the paper.

| Symbol | Meaning |
|---------------------|---|
| \mathcal{C} | Set of all clients ($N = \mathcal{C} $) |
| \mathcal{B} | Set of Byzantine clients ($M = \mathcal{B} $) |
| \mathcal{H} | Set of honest clients ($\mathcal{C} \setminus \mathcal{B}$) |
| ϵ | Fraction of adversarial clients ($\epsilon = M/N$) |
| w_t | Global model weights at round t |
| w_t^i | Local model weights of client i at round t |
| \mathcal{A} | Aggregation rule |
| D_i | Local dataset of client i |
| $n \leq N$ | Number of sampled clients per round |
| η | Learning rate for local training |
| α | Dirichlet parameter controlling data heterogeneity |
| \mathcal{G} | Generator model of the conditional GAN |
| \mathcal{D}_{w_t} | Discriminator of the conditional GAN, parameterized by global model w_t |
| D_{syn} | Synthetic dataset generated by \mathcal{G} |
| β | Byzantine aggregation heuristic parameter: <ul style="list-style-type: none"> • In TRIMAVG, β is the ratio of updates trimmed from each extreme. • In MULTIKRUM, β is the assumed fraction of malicious clients, used to determine how many updates to discard. |

Formally, a central server \mathcal{S} , coordinates the training process across a set of N clients, denoted as $\mathcal{C} = \{1, 2, \dots, N\}$, where each client $i \in \mathcal{C}$ possesses a private dataset, D_i . The global objective is to minimize the empirical risk over the union of all datasets:

$$\min_{w \in \mathbb{R}^d} f(w) = \sum_{i=1}^N \frac{|D_i|}{|D|} f_i(w), \quad f_i(w) = \frac{1}{|D_i|} \sum_{(x,y) \in D_i} \ell(w; x, y),$$

where w denotes model parameters, ℓ is the loss function, and $|D| = \sum_{i=1}^N |D_i|$.

Training proceeds iteratively: at each round t , the server samples a subset $\mathcal{C}_t \subseteq \mathcal{C}$ with $|\mathcal{C}_t| = n \leq N$ and broadcasts the current model w_t . Each selected client $i \in \mathcal{C}_t$ performs local updates to produce w_t^i , and the server aggregates them, typically via weighted averaging (FedAvg) [24]:

$$w_{t+1} = \frac{1}{K} \sum_{i \in \mathcal{C}_t} |D_i| w_t^i,$$

where $K = \sum_{i \in \mathcal{C}_t} |D_i|$.

2.2 Byzantine Threats in Federated Learning

Federated Learning (FL) is inherently vulnerable to *Byzantine clients*, participants that deviate from honest behavior due to

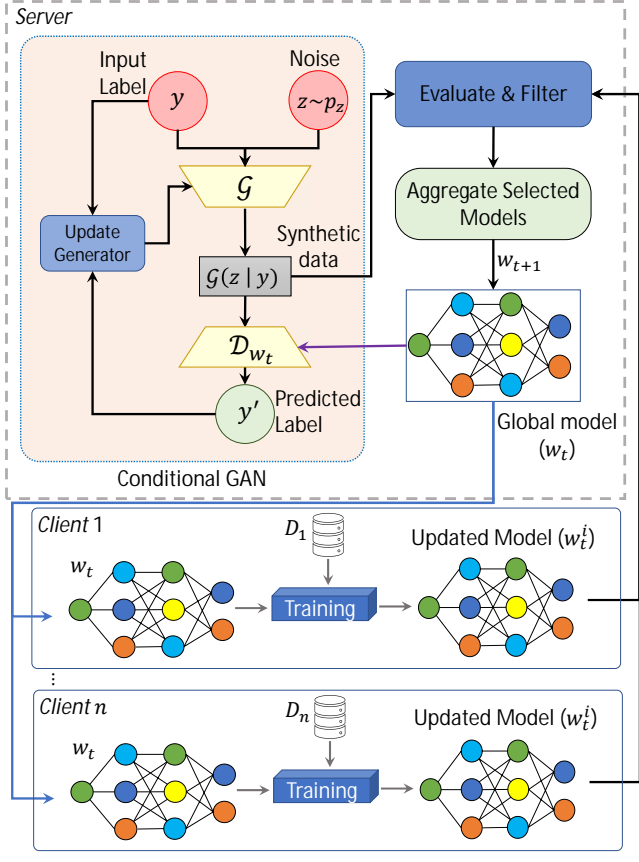


Figure 1: Proposed defense pipeline to authenticate updates.

malicious intent or faults. Such adversaries exploit the server’s implicit trust in client updates, where neither training data nor parameter integrity can be directly verified. This vulnerability is exacerbated in heterogeneous settings, where non-IID distributions naturally induce divergence among honest updates, providing camouflage for adversarial perturbations.

Byzantine threats typically manifest as *data poisoning*, where local datasets are tampered with (e.g., label flips or feature manipulations) to propagate misleading gradients [7, 34], or as *model poisoning*, where adversaries directly craft malicious parameter updates to bias or destabilize the global model [2, 12]. Attacks may be *untargeted*, aiming to degrade overall accuracy, or *targeted*, enforcing specific misclassifications. Their subtlety, often designed to mimic the variance of benign updates, poses a central challenge for detection, particularly against adaptive adversaries that evolve to evade robust aggregation mechanisms.

2.3 Defenses Against Byzantine Attacks

The problem of Byzantine threats in FL has received significant attention in the recent years and a number of defenses

have been proposed with various advantages and drawbacks. These defenses fall into two broad categories: *Robust aggregation mechanisms*, and *Filtration-based techniques*.

Robust aggregation mechanisms aim to reduce the impact of malicious updates during model aggregation by designing the Byzantine-robust aggregation rules that are resilient to outliers and adversarial manipulations. Popular examples include Coordinate-wise Median and Trimmed-Mean [38] [8, 22, 38], which respectively down-weight or exclude extreme coordinate values; Krum [3], which selects the update closest to the majority; Bulyan [25], which combines Krum and Trimmed-Mean; and RFA [30], which aggregates via the geometric median. While these rules improve resilience to outliers, their effectiveness degrades under large-scale collusion or adaptive attacks. Moreover, they are subject to fundamental error lower bounds [1, 19], which we discuss in Section 2.4.

Filtration-based techniques instead attempt to detect and exclude malicious updates before aggregation. One line of work uses clustering (e.g., Aurora [33], FoolsGold [14], Flame [29]) to identify anomalous updates, assuming benign clients form a coherent cluster. Another line relies on validation-based authentication, where updates are scored against a reference dataset (e.g., FLTrust [5], GAN-based validation [41]). More recent approaches (e.g., DeepSight [31], FedDMC [27]) extend these ideas with adversarial feature analysis or deep anomaly detection. While effective, filtration methods often depend on clean validation data or incur higher computational costs.

2.4 Limitations of Byzantine Defenses

Despite significant progress, existing defenses against Byzantine attacks in federated learning face fundamental limitations that constrain their robustness and scalability. Broadly, these limitations arise from both *practical trade-offs* in algorithm design and *theoretical lower bounds* that no aggregation-based defense can overcome.

From a practical perspective, aggregation rules often incur accuracy or efficiency penalties. For instance, Krum selects only one update per round, which significantly slows convergence [3]. Its variant, MultiKrum, requires prior knowledge of the number of malicious clients, an unrealistic assumption in practice. Trimmed Mean depends on heuristics to determine how many extreme values to discard, which can lead to under- or over-pruning depending on the distribution of updates [38]. Filtration-based defenses such as FLTrust [5] or the work by Li *et al.* [23] improve robustness by leveraging a clean reference dataset, but this reliance on external data limits scalability and privacy. Generative-data-based defenses, such as Zhao *et al.* [41], similarly use GANs for validation but still depend on centralized or external datasets for training.

Beyond these implementation-level trade-offs, there are also *irreducible theoretical limits* on the robustness of aggregation-based defenses. Recent results show that for any

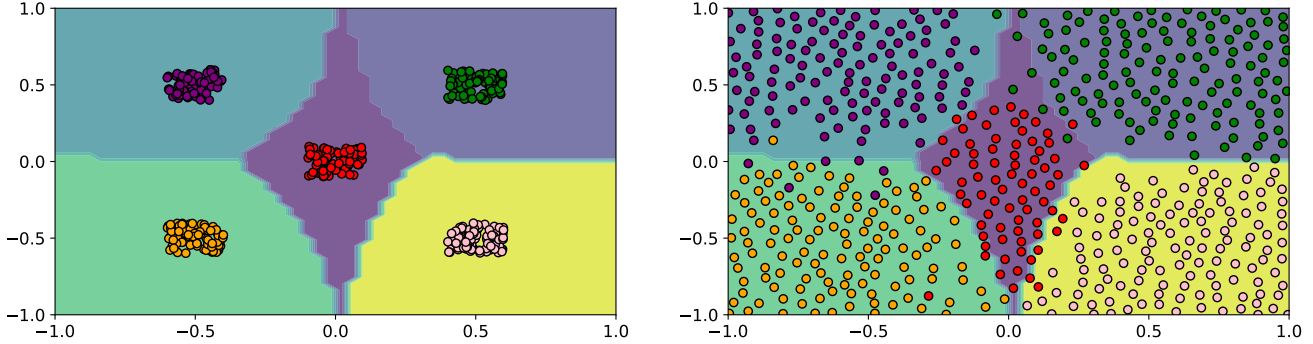


Figure 2: A 2D toy illustration of our approach. **Left:** the original dataset (points) and decision boundaries learned by a simple MLP. **Right:** synthetic data generated by our method, filtered so that each point is at least a minimum distance apart for clarity.

permutation-invariant aggregation rule, the expected optimization error under an ϵ fraction of Byzantine clients is bounded below by

$$\mathbb{E}[f(\hat{w}_t)] - f(w^*) \geq \Omega\left(\frac{\epsilon\sigma^2}{\mu}\right),$$

where μ denotes the strong convexity parameter and σ^2 the variance of the gradients [17, 18]. In heterogeneous data settings, the error can also be expressed as

$$\mathbb{E}[\|\hat{w} - \mu\|^2] \geq \epsilon\rho^2,$$

with ρ^2 bounding pairwise distances between honest updates. Strikingly, if the adversarial fraction $\epsilon \geq 1/2$, the error may even become unbounded, fundamentally limiting the efficacy of robust aggregation in highly adversarial regimes. These results demonstrate that robust-aggregation alone cannot circumvent a fundamental accuracy barrier.

Taken together, these findings underscore the inherent limitations of aggregation-centric defenses. Filtration-based approaches attempt to overcome these constraints by detecting and removing malicious updates, but they often depend on clean reference datasets or trusted validation, which can limit scalability and practicality. This combination of aggregation lower bounds and filtration dependencies motivates the exploration of alternative strategies.

In this work, we propose a generative-data-driven filtration mechanism that eliminates the need for external datasets while effectively mitigating the fundamental accuracy limits imposed on aggregation-based defenses. Specifically, by training a generator on the global model itself, our method leverages synthetic data to validate updates, circumventing the error lower bounds associated with aggregation-only rules while preserving privacy.

3 Problem Setup

In this section, we define the threat model considered in our work, describe the defense objectives guiding our framework,

and specify the assumptions made.

3.1 Threat Model

We consider the classical FL setup introduced in Section 2.1, where N clients collaboratively train a global model with parameters $w \in \mathbb{R}^d$ under the coordination of a central server S . A fraction ϵ of clients, denoted $\mathcal{B} \subseteq \mathcal{C}$, are controlled by an adversary, so that $|\mathcal{B}| = \epsilon N = M$.

The adversary aims to disrupt the training process by injecting malicious updates into the aggregation process. We assume a **non-omniscient** adversary with the following capabilities:

- **Local knowledge:** The adversary has access to the data, local updates, and training hyperparameters of compromised clients.
- **Aggregation awareness:** The adversary knows the server's aggregation rule and any deployed defense mechanism.
- **Limited visibility:** The adversary cannot access the raw data of honest clients, though it may observe their updates in certain adaptive attack scenarios.
- **Collusion:** Compromised clients may coordinate their strategies and leverage their own local datasets, similar to honest clients.

We assume the server behaves honestly, and compromised clients can manipulate only their own data and updates. This threat model captures realistic adversarial scenarios in federated learning, where malicious clients may collude yet cannot compromise honest participants or the server.

3.2 Defense Objectives

Motivated by the limitations of existing aggregation- and filtration-based defenses (Section 2.4), our framework is designed to achieve the following objectives:

1. **Robustness:** Preserve global model integrity under poisoning attacks, including adaptive and intermittent strategies.
2. **Generality:** Operate without prior knowledge of the number of adversaries M or the specific attack strategies.
3. **Fairness:** Minimize false rejection of benign client updates while preserving decision-boundary integrity

These objectives are achieved through a dynamic, synthetic-data-driven mechanism that probes the global model’s decision boundaries to detect malicious updates. The following section formalizes our defense framework, showing how boundary-aligned synthetic samples, generated without accessing client data, enable robustness, generality, and fairness in federated learning.

4 Defense Formulation

Our defense builds on the intuition that machine learning classifiers learn decision boundaries to separate data points into classes, while adversaries in poisoning attacks attempt to perturb these boundaries to degrade model performance. Effective defenses must therefore detect or neutralize such perturbations. Authentication-based methods provide a promising direction by validating client updates against a trusted reference; however, existing approaches require clean validation datasets, which is unrealistic in privacy-preserving FL.

We address this problem by re-purposing conditional Generative Adversarial Networks (cGANs) [26] to generate synthetic data aligned with the decision geometry of the global model, rather than replicating private distributions. Unlike prior GAN-based defenses that rely on auxiliary datasets, our method produces boundary-focused samples that may appear unrealistic to humans but remain meaningful to the model for detecting poisoned updates. Figure 2 illustrates this principle using a toy example: real data is clustered, whereas synthetic samples spread across the decision space along critical decision boundaries, providing informative probes for identifying malicious contributions.

To achieve this, we introduce three key modifications: (i) replacing the discriminator with the global model, (ii) training only the generator while keeping the global model fixed, and (iii) eliminating real/fake samples entirely, enabling fully data-free training. These changes yield boundary-aligned synthetic data that is independent of client distributions and serves as a trusted reference for update authentication. This approach directly addresses the robustness, generality, and fairness objectives by providing meaningful probes for detecting malicious contributions without exposing client data.

While more recent conditional GAN variants (e.g., cGAN [11]) could be explored, we use a standard cGAN in this work. This choice reflects both the preliminary nature of

Algorithm 1 Federated Learning with GAN-based Defense

Input:

| | |
|---------------|------------------------------|
| η | Learning rate |
| T | Total communication rounds |
| E | Number of local epochs |
| B | Batch size |
| \mathcal{A} | Server-side aggregation rule |

Output:

| | |
|---|----------------------|
| w_T | Trained global model |
| 1: $w_0 \leftarrow$ random initialization | |
| 2: for $t = 1, 2, \dots, T$ do | |
| 3: Randomly samples a set of n clients \mathcal{C} | |
| 4: Send w_{t-1} to all sampled clients | |
| 5: Client-side (in parallel): | |
| 6: for each $i \in \mathcal{C}$ do | |
| 7: $w_t^i \leftarrow$ LocalTraining(i, w_{t-1}, η, B, E) | |
| 8: Send w_t^i to server | |
| 9: end for | |
| 10: Server-side (in parallel): | |
| 11: Initialize discriminator $\mathcal{D}_{w_{t-1}}$ | |
| 12: Train generator \mathcal{G} of cGAN | |
| 13: Generate synthetic dataset D_{syn} using \mathcal{G} | |
| 14: Collect updates $\{w_t^i\}_{i \in \mathcal{C}}$ | |
| 15: $S_t \leftarrow$ FilterUpdates($\{w_t^i\}, D_{\text{syn}}$) | |
| 16: $w_t \leftarrow \mathcal{A}(\{w_t^j\}_{j \in S_t})$ | |
| 17: end for | |
| 18: return w_T | ▷ Final global model |

our study, focusing on validating the core defense concept, and practical considerations: standard cGANs provide a favorable balance between training complexity and computational resources, making them well-suited for large-scale federated experiments. In the next subsection, we detail the training procedure for the generator, showing how these modifications produce boundary-aligned synthetic data suitable for update authentication.

4.1 Training the Generator

Unlike conventional cGANs, our generator \mathcal{G} is trained not to deceive a binary discriminator, but to align with the decision boundaries of the global model w_t , ensuring synthetic data reflects the model’s current knowledge. Formally, given noise $z \sim p_z$ and labels $y \sim p_y$, \mathcal{G} produces synthetic samples $\mathcal{G}(z|y)$, which are evaluated by the global model \mathcal{D}_{w_t} . The generator is updated via the cross-entropy (CE) loss:

$$\min_{\mathcal{G}} \mathcal{L}_{\mathcal{G}} = \mathbb{E}_{z \sim p_z, y \sim p_y} [\ell(\mathcal{D}_{w_t}(\mathcal{G}(z|y)), y)] \quad (1)$$

Training proceeds by sampling (z, y) , generating $\mathcal{G}(z|y)$, evaluating $\mathcal{D}_{w_t}(\mathcal{G}(z|y))$, and updating \mathcal{G} by minimizing CE loss. This ensures that generated samples remain aligned with the classifier’s evolving decision regions.

Algorithm 2 Local model training of client i

Input:

w_t Global model
 η Learning rate
 B Batch size
 E Number of local epochs

Output:

w_t^i Updated local model
1: $w_t^i \leftarrow w_t$
2: **if** $i \in \mathcal{B}$ **then** ▷ Client i is malicious
3: $w_t^i \leftarrow \text{PoisonAttack}(w_t^i)$
4: **else** ▷ Client i is benign
5: **for** $e = 1, \dots, E$ **do**
6: Sample mini-batch $D \subset D_i$ of size B
7: $w_t^i \leftarrow w_t^i - \eta \nabla \ell(D, w_t^i)$
8: **end for**
9: **end if**
10: **return** w_t^i

Algorithm 3 Filtering client updates

Input:

m Filter (Fixed, Adaptive, Cluster)
 $\{w_t^i\}$ Set of client models
 D_{syn} Synthetic validation dataset
 $\text{EVAL}(\cdot)$ Evaluation function
 τ (optional) Threshold for Fixed method

Output:

S_t Set of accepted client models
1: Compute metrics: $\text{metrics}[w_t^i] \leftarrow \text{EVAL}(w_t^i, D_{\text{syn}})$, $\forall i$
2: Transform to scores (so that *higher = better*):

$$\text{score}[w] = \begin{cases} -\text{metrics}[w], & \text{if metric is loss} \\ +\text{metrics}[w], & \text{if metric is accuracy} \end{cases}$$

3: Initialize $S_t \leftarrow \emptyset$
4: **if** $m = \text{Fixed}$ **then**
5: $S_t \leftarrow \{w_t^i \mid \text{score}[w_t^i] > \tau\}$
6: **else if** $m = \text{Adaptive}$ **then**
7: $\tau \leftarrow \text{Mean}(\text{score})$
8: $S_t \leftarrow \{w_t^i \mid \text{score}[w_t^i] > \tau\}$
9: **else if** $m = \text{Cluster}$ **then**
10: Partition scores: $C_1, C_2 \leftarrow \text{K-Means}(\text{score}, 2)$
11: Identify best client: $w^+ \leftarrow \arg \max_i \text{score}[w_t^i]$
12: $S_t \leftarrow C_j$ s.t. $w^+ \in C_j$ ▷ Cluster with best client
13: **end if**
14: **return** S_t

4.2 Generating Synthetic Data

After training, the generator produces a synthetic validation set

$$D_{\text{syn}} = \{(X_i, Y_i)\}_{i=1}^K,$$

with $K = q \cdot C$, where C is the number of classes and q is the number of per-class samples. Although these synthetic points may not resemble raw inputs, they populate the decision boundaries that are most susceptible to adversarial manipulation, making them effective for validating model updates.

4.3 Authentication of Model Updates

The server uses D_{syn} as a trusted reference to authenticate client updates. Each update w_t^i is evaluated on D_{syn} using a metric \mathcal{F} (e.g., accuracy or loss). Updates are then filtered using either threshold-based or clustering-based methods.

In the fixed threshold variant, w_t^i is accepted if $\mathcal{F}(w_t^i; D_{\text{syn}}) > \tau$, where τ is a constant. Adaptive thresholds adjust τ_t dynamically (e.g., setting it to the mean or median of the current round's metrics), improving resilience against evolving attacks. Alternatively, clustering-based methods (e.g., K-Means) group updates by their performance on D_{syn} and flag outliers as malicious.

Algorithm 3 summarizes the filtering process. While our evaluation shows adaptive thresholds provide the best trade-off, the framework is agnostic: any authentication method requiring a validation set can operate on D_{syn} , without assuming access to clean external data.

5 Experimental Setting

We evaluate our framework on widely used image classification datasets, implement several representative poisoning attacks, compare against state-of-the-art baselines, and report standard evaluation metrics. All attacks and defenses are implemented according to their original designs, using provided code when available.

5.1 Datasets and Model

We consider three benchmark datasets:

- **MNIST** [10]: 28×28 grayscale handwritten digits (60,000 training, 10,000 test samples).
- **Fashion-MNIST (FMNIST)** [36]: 28×28 grayscale images of clothing items (60,000 training, 10,000 test samples).
- **CIFAR-10** [20]: 32×32 RGB images across 10 classes (50,000 training, 10,000 test samples).

We use LeNet-5 [21] for MNIST and FMNIST, and ResNet-18 [15] for CIFAR-10. To simulate statistical heterogeneity, data is partitioned among clients using a class-wise Dirichlet distribution [18, 39], with concentration parameter α . We evaluate four regimes: (i) near-IID ($\alpha = 100$), (ii) low non-IID ($\alpha = 10$), (iii) moderate non-IID ($\alpha = 1$), and (iv) extreme

non-IID ($\alpha = 0.1$). Results for the near-IID case ($\alpha = 100.0$) and the extreme non-IID case ($\alpha = 0.1$) are presented in the main body, while intermediate settings ($\alpha = 10.0, 1.0$) are reported in Appendix B.

5.2 System Setup

We consider 100 clients in total, of which a subset may be malicious. In each communication round, 10 clients are randomly selected to perform 10 local epochs of training using SGD with a learning rate of 0.01 and a batch size of 128. The updated models are then submitted to the server for aggregation. This process is repeated for 200 global communication rounds. Additional hyperparameters and setup details are provided in Appendix A.

5.3 Attack Setup

To evaluate the robustness of our framework, we implement the following poisoning attacks:

- **Random Noise (RN)**: Malicious clients submit random updates sampled from a normal distribution.
- **Sign Flipping (SF)** [19]: Clients invert the sign of their gradient updates, effectively performing gradient ascent.
- **Label-Flipping (LF)** [13]: Clients flip the labels of their local training data to degrade global model performance.
- **Inner Product Manipulation (IPM)**: Clients manipulate gradient directions to maximize divergence from the benign average.

We vary the malicious client proportion in $\{10\%, 20\%, 30\%\}$, consistent with prior federated learning threat models [32]. By default, adversaries behave maliciously in every selected round.

5.4 Compared Baselines

We compare our method against widely recognized aggregation strategies:

- **FEDAVG** [24]: Standard averaging of client updates.
- **MEDIAN** [38]: Coordinate-wise median to mitigate outliers.
- **Geometric Median (GEOMEDIAN)** [30]: Aggregation via geometric median for Byzantine robustness.
- **Trimmed Mean (TRIMAVG)** [38]: Removes extreme updates before averaging.
- **MULTIKRUM** [3]: Selects updates most similar to others for aggregation.

- **Nearest Neighbor Mixing (NNM+KRUM)** [1]: Combines nearest-neighbor filtering with Krum aggregation.
- **Nearest Neighbor Mixing (NNM+KRUM)** [1]: A two-step robust aggregation method that first smooths client updates using nearest-neighbor averaging to mitigate the effect of outliers, and then applies Krum to select the update closest to the majority.

These baselines cover both statistical heterogeneity and adversarial robustness, providing a comprehensive set of comparisons.

5.5 Evaluation Metrics

We report the following metrics:

- **Main Task Accuracy (ACC)**: Accuracy of the global model on a clean test set, reflecting primary task performance.
- **True Positive Rate (TPR)**: Fraction of malicious updates correctly identified:

$$TPR = \frac{TP}{TP + FN},$$

where TP is the number of malicious models correctly detected, and FN the number missed.

- **True Negative Rate (TNR)**: Fraction of benign updates correctly identified:

$$TNR = \frac{TN}{TN + FP},$$

where TN is the number of benign models correctly accepted, and FP the number falsely flagged as malicious.

These metrics together measure task accuracy, attack resilience, and detection effectiveness [1, 28].

6 Experimental Results

We compare our method against state-of-the-art baselines under various adversarial settings and analyze its performance using the evaluation metrics described in Section 5.5. Results across datasets and poisoning scenarios consistently show that our GAN-based defenses achieve both high task accuracy and strong detection performance, outperforming standard aggregation rules.

6.1 Robustness Against Poisoning Attacks

We evaluate robustness against the four poisoning attacks from Section 5.3. Across datasets, conventional methods (FEDAVG, MEDIAN, TRIMAVG, GEOMEDIAN, MULTIKRUM, NNM+KRUM) perform well without adversaries

Table 2: Overall test accuracy (ACC) of federated learning under benign training and poisoning attacks across malicious client fractions (10%, 20%, 30%) in the near-IID setting $\alpha = 100$. Results are reported on MNIST, Fashion-MNIST, and CIFAR-10, comparing standard aggregation rules (FEDAVG, MEDIAN, TRIMMED MEAN, GEOMEDIAN, KRUM, NNM+KRUM) against our proposed GAN-based authentication variants. GAN-based defenses consistently preserve accuracy even under high adversarial presence, whereas conventional robust aggregation methods degrade significantly.

| Baseline | No Attack | $\epsilon = 10\%$ | | | | $\epsilon = 20\%$ | | | | $\epsilon = 30\%$ | | | | |
|---------------|-----------------------|-------------------|------|------|------|-------------------|------|------|------|-------------------|------|------|------|------|
| | | RN | LF | SF | IPM | RN | LF | SF | IPM | RN | LF | SF | IPM | |
| MNIST | FEDAVG | 0.99 | 0.88 | 0.98 | 0.11 | 0.11 | 0.54 | 0.11 | 0.11 | 0.11 | 0.10 | 0.11 | 0.10 | 0.10 |
| | MEDIAN | 0.99 | 0.99 | 0.99 | 0.99 | 0.99 | 0.90 | 0.11 | 0.99 | 0.10 | 0.10 | 0.11 | 0.11 | 0.10 |
| | TRIMAVG | 0.99 | 0.91 | 0.99 | 0.98 | 0.11 | 0.85 | 0.97 | 0.95 | 0.10 | 0.10 | 0.11 | 0.11 | 0.10 |
| | GEOMEDIAN | 0.99 | 0.99 | 0.99 | 0.99 | 0.99 | 0.96 | 0.98 | 0.99 | 0.10 | 0.10 | 0.11 | 0.11 | 0.10 |
| | MULTIKRUM | 0.99 | 0.94 | 0.99 | 0.98 | 0.11 | 0.40 | 0.98 | 0.11 | 0.10 | 0.10 | 0.11 | 0.11 | 0.10 |
| | NNM+KRUM | 0.99 | 0.93 | 0.99 | 0.98 | 0.11 | 0.89 | 0.95 | 0.11 | 0.10 | 0.10 | 0.11 | 0.11 | 0.10 |
| | GAN (FIXED THRESHOLD) | 0.99 | 0.99 | 0.99 | 0.99 | 0.99 | 0.99 | 0.99 | 0.99 | 0.99 | 0.99 | 0.99 | 0.99 | 0.99 |
| Fashion MNIST | GAN (ADAPTIVE: MEAN) | 0.99 | 0.99 | 0.99 | 0.99 | 0.99 | 0.99 | 0.99 | 0.99 | 0.99 | 0.99 | 0.99 | 0.99 | 0.99 |
| | GAN (CLUSTERED) | 0.99 | 0.99 | 0.99 | 0.99 | 0.99 | 0.99 | 0.99 | 0.99 | 0.99 | 0.99 | 0.99 | 0.99 | 0.99 |
| | FEDAVG | 0.89 | 0.71 | 0.89 | 0.10 | 0.10 | 0.27 | 0.86 | 0.10 | 0.10 | 0.10 | 0.10 | 0.10 | 0.10 |
| | MEDIAN | 0.89 | 0.89 | 0.88 | 0.88 | 0.89 | 0.76 | 0.80 | 0.87 | 0.10 | 0.10 | 0.10 | 0.10 | 0.10 |
| | TRIMAVG | 0.89 | 0.66 | 0.88 | 0.79 | 0.10 | 0.69 | 0.81 | 0.10 | 0.10 | 0.10 | 0.10 | 0.10 | 0.10 |
| | GEOMEDIAN | 0.89 | 0.88 | 0.89 | 0.88 | 0.89 | 0.84 | 0.86 | 0.87 | 0.10 | 0.10 | 0.10 | 0.10 | 0.10 |
| | MULTIKRUM | 0.89 | 0.78 | 0.89 | 0.10 | 0.10 | 0.71 | 0.88 | 0.10 | 0.10 | 0.10 | 0.10 | 0.10 | 0.10 |
| CIFAR-10 | NNM+KRUM | 0.89 | 0.77 | 0.89 | 0.10 | 0.10 | 0.72 | 0.87 | 0.10 | 0.10 | 0.10 | 0.10 | 0.10 | 0.10 |
| | GAN (FIXED THRESHOLD) | 0.89 | 0.89 | 0.89 | 0.89 | 0.89 | 0.89 | 0.89 | 0.89 | 0.89 | 0.88 | 0.88 | 0.88 | 0.88 |
| | GAN (ADAPTIVE: MEAN) | 0.89 | 0.89 | 0.89 | 0.89 | 0.89 | 0.89 | 0.89 | 0.89 | 0.89 | 0.89 | 0.89 | 0.88 | 0.89 |
| | GAN (CLUSTERED) | 0.89 | 0.89 | 0.89 | 0.89 | 0.89 | 0.89 | 0.89 | 0.89 | 0.89 | 0.89 | 0.89 | 0.88 | 0.89 |
| | FEDAVG | 0.88 | 0.12 | 0.88 | 0.59 | 0.10 | 0.11 | 0.86 | 0.10 | 0.10 | 0.11 | 0.60 | 0.10 | 0.10 |
| | MEDIAN | 0.88 | 0.87 | 0.88 | 0.86 | 0.86 | 0.44 | 0.86 | 0.82 | 0.10 | 0.13 | 0.83 | 0.72 | 0.10 |
| | TRIMAVG | 0.89 | 0.13 | 0.87 | 0.82 | 0.27 | 0.12 | 0.86 | 0.75 | 0.44 | 0.13 | 0.84 | 0.63 | 0.10 |
| CIFAR-10 | GEOMEDIAN | 0.89 | 0.88 | 0.88 | 0.87 | 0.87 | 0.43 | 0.87 | 0.84 | 0.10 | 0.13 | 0.86 | 0.76 | 0.10 |
| | MULTIKRUM | 0.89 | 0.13 | 0.88 | 0.82 | 0.10 | 0.15 | 0.88 | 0.79 | 0.17 | 0.15 | 0.85 | 0.76 | 0.30 |
| | NNM+KRUM | 0.89 | 0.13 | 0.88 | 0.82 | 0.10 | 0.13 | 0.87 | 0.80 | 0.18 | 0.12 | 0.84 | 0.77 | 0.10 |
| | GAN (FIXED THRESHOLD) | 0.56 | 0.58 | 0.56 | 0.56 | 0.56 | 0.57 | 0.57 | 0.57 | 0.57 | 0.56 | 0.57 | 0.56 | 0.57 |
| | GAN (ADAPTIVE: MEAN) | 0.88 | 0.88 | 0.88 | 0.88 | 0.88 | 0.88 | 0.88 | 0.88 | 0.88 | 0.87 | 0.87 | 0.88 | 0.88 |
| | GAN (CLUSTERED) | 0.88 | 0.88 | 0.88 | 0.88 | 0.88 | 0.88 | 0.88 | 0.88 | 0.88 | 0.87 | 0.87 | 0.87 | 0.87 |

*we set $\beta = 0.1, 0.2, 0.3$ (where β is byzantine aggregation heuristic, for TRIMAVG and MULTIKRUM respectively under 10%, 20%, and 30% malicious clients.

but degrade sharply once malicious clients are introduced. For instance, under Sign Flipping with 30% adversaries on MNIST, FEDAVG and KRUM collapse to 10% accuracy, while our adaptive GAN variants sustain 99%. Robust baselines such as TRIMAVG and GEOMEDIAN resist simple attacks but fail under stronger ones (e.g., IPM). In contrast, GAN-based defenses consistently maintain high ACC while neutralizing diverse poisoning strategies.

6.2 Impact of Statistical Heterogeneity

To study statistical heterogeneity, we partition data using a class-wise Dirichlet distribution with concentration parameter α . We evaluate four regimes: near-IID ($\alpha = 100$), low

heterogeneity ($\alpha = 10$), moderate heterogeneity ($\alpha = 1$), and extreme heterogeneity ($\alpha = 0.1$).

Table 2 (near-IID) and Table 3 (extreme non-IID) capture the extremes. In the near-IID case, all methods start with high baseline accuracy, yet standard defenses degrade rapidly as the adversarial fraction grows. In the extreme case ($\alpha = 0.1$), degradation is severe: FEDAVG and KRUM collapse, and robust baselines lose effectiveness. By contrast, our adaptive GANs preserve high accuracy even at $\epsilon = 30\%$, demonstrating resilience to both non-IID data and adversarial pressure. Notably, under benign IID conditions, the fixed-threshold variant achieves near-perfect performance (e.g., ACC=0.99 on MNIST with 30% malicious clients; Table 2), effectively mit-

Table 3: Overall test accuracy (ACC) of federated learning under benign training and poisoning attacks across malicious client fractions (10%, 20%, 30%) in the extreme non-IID setting $\alpha = 0.1$. Results are reported on MNIST, Fashion-MNIST, and CIFAR-10, comparing standard aggregation rules (FEDAVG, MEDIAN, TRIMMED MEAN, GEOMEDIAN, KRUM, NNM+KRUM) against our proposed GAN-based authentication variants. GAN-based defenses consistently preserve accuracy even under high adversarial presence, whereas conventional robust aggregation methods degrade significantly.

| Baseline | No Attack | $\epsilon = 10\%$ | | | | $\epsilon = 20\%$ | | | | $\epsilon = 30\%$ | | | |
|---------------|-----------------------|-------------------|------|------|------|-------------------|------|------|------|-------------------|------|------|------|
| | | RN | LF | SF | IPM | RN | LF | SF | IPM | RN | LF | SF | IPM |
| MNIST | FEDAVG | 0.99 | 0.17 | 0.95 | 0.10 | 0.10 | 0.17 | 0.67 | 0.10 | 0.10 | 0.10 | 0.10 | 0.10 |
| | MEDIAN | 0.98 | 0.98 | 0.98 | 0.98 | 0.98 | 0.64 | 0.98 | 0.97 | 0.10 | 0.10 | 0.96 | 0.10 |
| | TRIMAVG | 0.98 | 0.43 | 0.98 | 0.96 | 0.10 | 0.14 | 0.98 | 0.10 | 0.10 | 0.10 | 0.96 | 0.11 |
| | GEOMEDIAN | 0.99 | 0.99 | 0.99 | 0.99 | 0.98 | 0.64 | 0.99 | 0.97 | 0.10 | 0.10 | 0.98 | 0.11 |
| | MULTIKRUM | 0.96 | 0.53 | 0.97 | 0.10 | 0.10 | 0.33 | 0.87 | 0.10 | 0.11 | 0.10 | 0.11 | 0.10 |
| | NNM+KRUM | 0.98 | 0.37 | 0.98 | 0.94 | 0.10 | 0.24 | 0.97 | 0.10 | 0.10 | 0.10 | 0.97 | 0.11 |
| Fashion MNIST | GAN (FIXED THRESHOLD) | 0.62 | 0.65 | 0.64 | 0.59 | 0.58 | 0.62 | 0.65 | 0.68 | 0.64 | 0.54 | 0.79 | 0.58 |
| | GAN (ADAPTIVE: MEAN) | 0.98 | 0.96 | 0.97 | 0.97 | 0.98 | 0.93 | 0.98 | 0.98 | 0.98 | 0.91 | 0.11 | 0.98 |
| | GAN (CLUSTERED) | 0.98 | 0.97 | 0.98 | 0.99 | 0.11 | 0.79 | 0.97 | 0.94 | 0.98 | 0.96 | 0.11 | 0.98 |
| | FEDAVG | 0.85 | 0.20 | 0.66 | 0.10 | 0.10 | 0.23 | 0.10 | 0.10 | 0.10 | 0.10 | 0.10 | 0.10 |
| | MEDIAN | 0.83 | 0.82 | 0.83 | 0.80 | 0.80 | 0.31 | 0.78 | 0.70 | 0.10 | 0.10 | 0.78 | 0.10 |
| | TRIMAVG | 0.85 | 0.28 | 0.85 | 0.10 | 0.10 | 0.38 | 0.78 | 0.10 | 0.10 | 0.10 | 0.77 | 0.10 |
| CIFAR-10 | GEOMEDIAN | 0.86 | 0.84 | 0.85 | 0.84 | 0.77 | 0.56 | 0.82 | 0.74 | 0.10 | 0.10 | 0.80 | 0.10 |
| | MULTIKRUM | 0.83 | 0.41 | 0.81 | 0.10 | 0.10 | 0.10 | 0.79 | 0.10 | 0.10 | 0.10 | 0.74 | 0.10 |
| | NNM+KRUM | 0.85 | 0.51 | 0.83 | 0.10 | 0.10 | 0.40 | 0.80 | 0.10 | 0.10 | 0.10 | 0.72 | 0.10 |
| | GAN (FIXED THRESHOLD) | 0.33 | 0.35 | 0.45 | 0.33 | 0.36 | 0.32 | 0.31 | 0.35 | 0.41 | 0.29 | 0.33 | 0.32 |
| | GAN (ADAPTIVE: MEAN) | 0.10 | 0.10 | 0.10 | 0.10 | 0.10 | 0.55 | 0.10 | 0.10 | 0.10 | 0.10 | 0.10 | 0.10 |
| | GAN (CLUSTERED) | 0.10 | 0.62 | 0.10 | 0.10 | 0.10 | 0.48 | 0.10 | 0.10 | 0.83 | 0.10 | 0.10 | 0.83 |

*we set $\beta = 0.1, 0.2, 0.3$ (where β is byzantine aggregation heuristic, for TRIMAVG and MULTIKRUM respectively under 10%, 20%, and 30% malicious clients.

igating Random Noise, Sign Flipping, Label-Flipping, and IPM attacks.

6.3 Intermediate Settings

In low and moderate non-IID regimes (Table 12 and Table 13 respectively), trends mirror those at the extremes: baseline methods rapidly degrade as heterogeneity and adversarial proportion increase, while GAN-based defenses remain stable. For instance, with $\alpha = 10$ and $\epsilon = 30\%$, FEDAVG accuracy drops to 10%, and KRUM also collapses to 10%, whereas our adaptive GAN maintains 99%. Similarly, at $\alpha = 1.0$, the fixed-threshold GAN sustains above 99% accuracy even under 30% adversaries, while conventional defenses fall below 10%.

Among our variants, the fixed-threshold GAN is conservative but steady, whereas the adaptive and clustered GANs achieve the best balance of accuracy and adaptability, consistently outperforming existing baselines across both intermediate settings.

6.4 Performance Under Benign Settings

To ensure defenses do not degrade normal learning, we evaluate ACC in the absence of malicious clients. On MNIST, Fashion-MNIST, and CIFAR-10, our methods achieve competitive accuracy under both IID ($\alpha = 100.0$) and non-IID ($\alpha = 0.1$) conditions (first column of Tables 2–13), confirming that robustness is not attained at the expense of benign

Table 4: True Positive Rate (TPR) of all evaluated defense methods across datasets and malicious client ratios, shown for Dirichlet $\alpha = 100$. Higher values indicate stronger detection of malicious updates.

| Baseline | No Attack | $\epsilon = 10\%$ | | | | $\epsilon = 20\%$ | | | | $\epsilon = 30\%$ | | | | |
|----------|-----------------------|-------------------|------|------|------|-------------------|------|------|------|-------------------|------|------|------|------|
| | | RN | LF | SF | IPM | RN | LF | SF | IPM | RN | LF | SF | IPM | |
| MNIST | MULTIKRUM | 0.00 | 0.68 | 0.67 | 0.67 | 0.68 | 0.64 | 0.74 | 0.75 | 0.42 | 0.33 | 0.70 | 0.72 | 0.28 |
| | GAN (FIXED THRESHOLD) | 0.00 | 1.00 | 1.00 | 1.00 | 1.00 | 1.00 | 1.00 | 1.00 | 1.00 | 1.00 | 1.00 | 1.00 | 1.00 |
| | GAN (ADAPTIVE: MEAN) | 0.00 | 1.00 | 1.00 | 1.00 | 1.00 | 1.00 | 1.00 | 1.00 | 1.00 | 1.00 | 1.00 | 1.00 | 1.00 |
| | GAN (CLUSTERED) | 0.00 | 1.00 | 1.00 | 1.00 | 1.00 | 1.00 | 1.00 | 1.00 | 1.00 | 1.00 | 1.00 | 1.00 | 1.00 |
| FMNIST | MULTIKRUM | 0.00 | 0.68 | 0.68 | 0.60 | 0.54 | 0.73 | 0.74 | 0.75 | 0.32 | 0.33 | 0.65 | 0.63 | 0.29 |
| | GAN (FIXED THRESHOLD) | 0.00 | 1.00 | 1.00 | 1.00 | 1.00 | 1.00 | 1.00 | 1.00 | 1.00 | 1.00 | 1.00 | 1.00 | 1.00 |
| | GAN (ADAPTIVE: MEAN) | 0.00 | 1.00 | 1.00 | 1.00 | 1.00 | 1.00 | 1.00 | 1.00 | 1.00 | 1.00 | 1.00 | 1.00 | 1.00 |
| | GAN (CLUSTERED) | 0.00 | 1.00 | 1.00 | 1.00 | 1.00 | 1.00 | 1.00 | 1.00 | 1.00 | 1.00 | 1.00 | 1.00 | 1.00 |
| CIFAR-10 | MULTIKRUM | 0.00 | 0.68 | 0.68 | 0.68 | 0.57 | 0.73 | 0.75 | 0.76 | 0.71 | 0.70 | 0.76 | 0.83 | 0.53 |
| | GAN (FIXED THRESHOLD) | 0.00 | 1.00 | 1.00 | 1.00 | 1.00 | 1.00 | 1.00 | 1.00 | 1.00 | 1.00 | 1.00 | 1.00 | 1.00 |
| | GAN (ADAPTIVE: MEAN) | 0.00 | 1.00 | 1.00 | 1.00 | 1.00 | 1.00 | 1.00 | 1.00 | 1.00 | 1.00 | 1.00 | 1.00 | 1.00 |
| | GAN (CLUSTERED) | 0.00 | 1.00 | 1.00 | 1.00 | 1.00 | 1.00 | 1.00 | 1.00 | 1.00 | 1.00 | 1.00 | 1.00 | 1.00 |

Table 5: True Negative Rate (TNR) of all evaluated defense methods across datasets and malicious client ratios, shown for Dirichlet $\alpha = 100$. Higher values indicate better preservation of benign updates.

| Baseline | No Attack | $\epsilon = 10\%$ | | | | $\epsilon = 20\%$ | | | | $\epsilon = 30\%$ | | | | |
|----------|-----------------------|-------------------|------|------|------|-------------------|------|------|------|-------------------|------|------|------|------|
| | | RN | LF | SF | IPM | RN | LF | SF | IPM | RN | LF | SF | IPM | |
| MNIST | MULTIKRUM | 1.00 | 0.96 | 0.96 | 0.96 | 0.96 | 0.90 | 0.92 | 0.93 | 0.85 | 0.71 | 0.86 | 0.87 | 0.69 |
| | GAN (FIXED THRESHOLD) | 0.99 | 1.00 | 0.99 | 1.00 | 0.88 | 0.99 | 0.98 | 1.00 | 1.00 | 0.99 | 0.98 | 1.00 | 0.99 |
| | GAN (ADAPTIVE: MEAN) | 0.79 | 0.91 | 0.91 | 0.91 | 0.91 | 0.95 | 0.95 | 0.95 | 0.95 | 0.98 | 0.98 | 0.98 | 0.98 |
| | GAN (CLUSTERED) | 0.85 | 0.93 | 0.94 | 0.94 | 0.93 | 0.97 | 0.97 | 0.97 | 0.97 | 0.98 | 0.98 | 0.98 | 0.98 |
| FMNIST | MULTIKRUM | 1.00 | 0.96 | 0.96 | 0.95 | 0.95 | 0.92 | 0.92 | 0.93 | 0.83 | 0.71 | 0.84 | 0.83 | 0.70 |
| | GAN (FIXED THRESHOLD) | 0.81 | 0.79 | 0.79 | 0.77 | 0.79 | 0.79 | 0.48 | 0.79 | 0.78 | 0.82 | 0.80 | 0.80 | 0.80 |
| | GAN (ADAPTIVE: MEAN) | 0.74 | 0.79 | 0.81 | 0.78 | 0.78 | 0.81 | 0.83 | 0.81 | 0.80 | 0.85 | 0.84 | 0.82 | 0.84 |
| | GAN (CLUSTERED) | 0.78 | 0.80 | 0.83 | 0.80 | 0.81 | 0.84 | 0.85 | 0.85 | 0.88 | 0.87 | 0.88 | 0.87 | 0.86 |
| CIFAR-10 | MULTIKRUM | 1.00 | 0.96 | 0.96 | 0.96 | 0.95 | 0.92 | 0.93 | 0.93 | 0.92 | 0.86 | 0.88 | 0.91 | 0.79 |
| | GAN (FIXED THRESHOLD) | 0.03 | 0.03 | 0.03 | 0.03 | 0.03 | 0.03 | 0.03 | 0.03 | 0.03 | 0.03 | 0.03 | 0.03 | 0.03 |
| | GAN (ADAPTIVE: MEAN) | 0.60 | 0.83 | 0.83 | 0.83 | 0.83 | 0.92 | 0.91 | 0.92 | 0.92 | 0.96 | 0.96 | 0.96 | 0.96 |
| | GAN (CLUSTERED) | 0.68 | 0.87 | 0.86 | 0.87 | 0.86 | 0.93 | 0.93 | 0.93 | 0.94 | 0.97 | 0.96 | 0.96 | 0.96 |

performance.

6.5 Detection Performance

Beyond accuracy, we assess the detection ability of our framework in terms of True Positive Rate (TPR) and True Negative Rate (TNR), which measure how effectively malicious updates are identified while preserving benign contributions. We compare against MULTIKRUM, a widely used Byzantine-resilient baseline that also performs selective aggregation.

Our adaptive-threshold variants achieve near-perfect de-

tection of malicious clients. On MNIST with 10% malicious clients, the adaptive method maintains a TPR between 0.98–1.00 across all attack types, compared to 0.54–0.68 for MULTIKRUM. Even under stronger adversarial pressure (30% malicious clients), and extreme heterogeneity ($\alpha = 0.1$) the adaptive GAN achieves a TPR of 0.88, outperforming MULTIKRUM (TPR = 0.31). Similar patterns hold across datasets: on CIFAR-10 with 20% malicious clients, the adaptive GAN sustains TPR ≈ 0.97 while MULTIKRUM drops below 0.20. Detailed TPR results for all datasets, malicious ratios, and Dirichlet distributions are provided in Tables 4, 6, 8, 10 in the

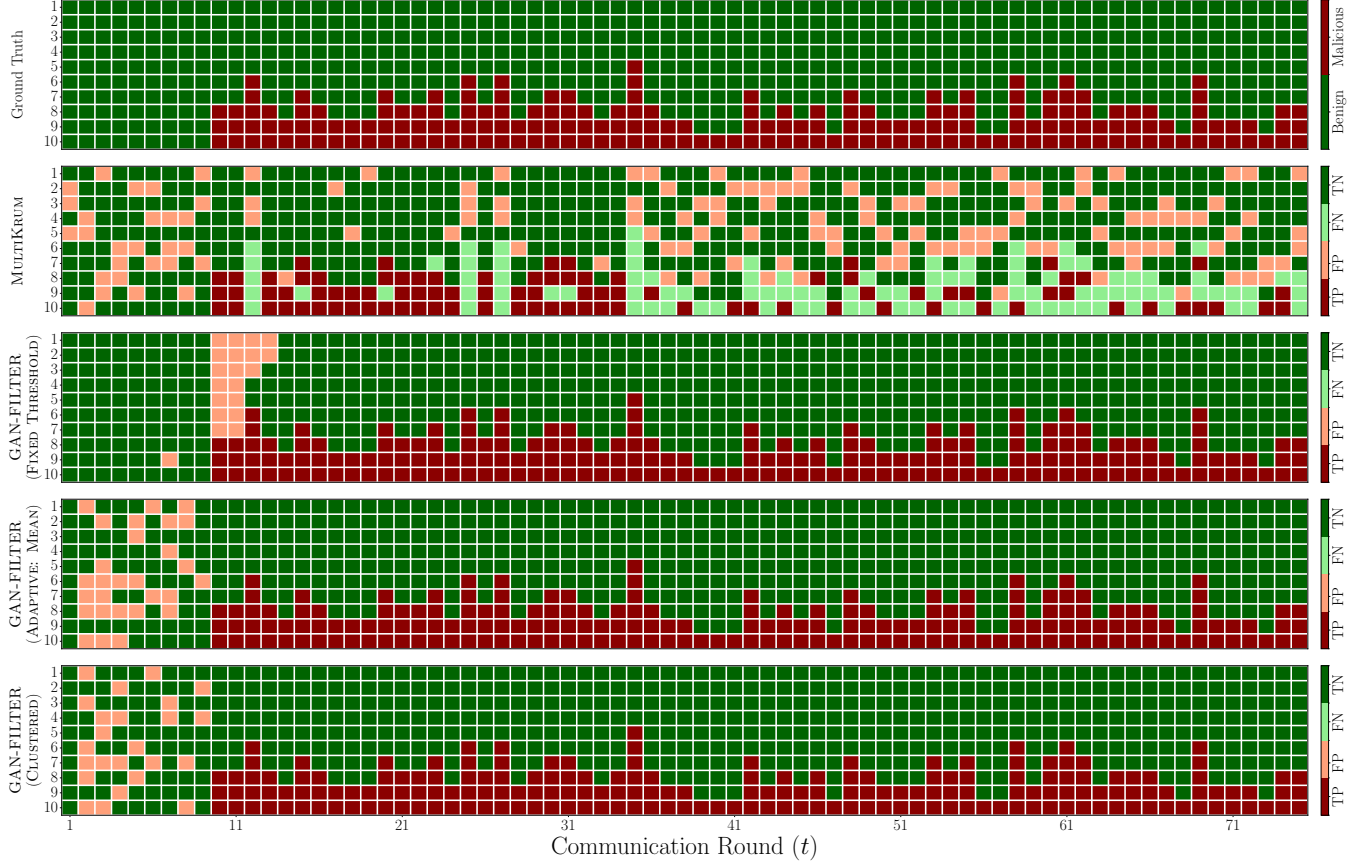


Figure 3: Heatmap of detection performance for MULTIKRUM and proposed variants under a Random Noise attack (30% malicious clients) on the MNIST dataset. The proposed GAN-based framework achieves high TPR and TNR, outperforming MULTIKRUM in detecting malicious updates.

Appendix B. Note that the True Positive Rate (TPR) is 0 in the absence of malicious clients, since there are no positive cases to detect.

The framework also preserves benign updates with high accuracy. On Fashion-MNIST with 30% malicious clients, adaptive and clustered variants achieve TNR in the range of 0.82–0.85, compared to 0.70–0.84 for MULTIKRUM. Full TNR results are reported in Tables 5, 7, 9, 11 in the Appendix B. Even in non-IID regimes, both TPR and TNR remain high, underscoring robustness to statistical heterogeneity.

Thresholding strategies. We observe that fixed-threshold filtering is less reliable, particularly on more complex datasets such as CIFAR-10. The difficulty lies in determining an appropriate universal threshold: what works for one dataset or attack setting often under- or over-filters in another. In contrast, adaptive and clustering strategies automatically adjust to the distribution of client performance, yielding more consistent detection. While our framework produces the synthetic dataset used for evaluation, the choice of thresholding strat-

egy ultimately lies with the deployer depending on system requirements and operational context.

To further illustrate these trends, the MNIST TPR/TNR heatmap under Random Noise attacks with 30% malicious clients is shown in Figure 3, while heatmaps for Fashion-MNIST and CIFAR-10 are provided in Appendix B. For clarity, only the first 75 communication rounds (out of 200) are displayed. Across datasets, our GAN-based defenses consistently outperform MULTIKRUM, achieving higher detection rates for adversarial updates while better preserving benign contributions.

A subtle trade-off arises in adversary-free scenarios: the adaptive strategy, by design, always filters a fraction of updates, which slightly lowers TNR due to increased false positives. However, fixed-threshold and clustering-based variants are less affected, and accuracy remains competitive. This highlights a tunable balance between conservativeness (fixed) and adaptability (adaptive), depending on deployment requirements.

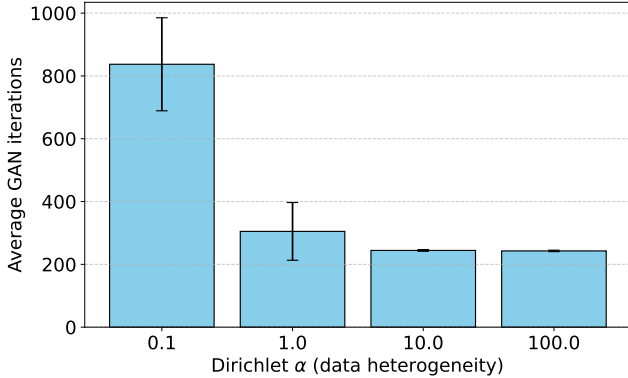


Figure 4: Average number of GAN training iterations required for the generator to reach early stopping across different Dirichlet α values. Smaller α corresponds to higher non-IID heterogeneity among clients. The plot shows that as α decreases (more heterogeneous data), the GAN requires more iterations on average, while IID settings (larger α) lead to faster convergence.

6.6 Training Efficiency of the GAN Defense

We analyze the evolution of GAN training overhead across communication rounds. The number of iterations required for stable generator convergence is highest during the early rounds of FL training and decreases sharply as the global model stabilizes. Early in training, the global model parameters are far from convergence, resulting in larger changes per round and requiring more effort from the framework to learn the evolving decision boundaries. As the model approaches stability, the GAN converges in fewer iterations. This reduction is more pronounced in IID settings, where client updates quickly cluster around the global model trajectory, whereas non-IID settings exhibit a slower decline due to higher variance and overlapping distributions. Overall, the amortized cost of deploying the GAN defense diminishes over time, making it practical for long-horizon FL training.

To quantify this effect, we group experiments by their Dirichlet α parameter and report the average number of GAN training iterations until convergence (Figure 4). The results confirm that overhead is significantly lower in IID regimes (large α), while non-IID cases (small α) consistently require more iterations due to heterogeneous updates.

We further examine GAN dynamics across communication rounds on the CIFAR-10 dataset for representative α values (Figure 5). The number of iterations needed to reach early stopping decreases steadily as FL training progresses. Near-IID settings ($\alpha = 100$) show a sharp decline, while non-IID settings (smaller α) maintain higher iterations for longer. These trends highlight that the amortized GAN training cost diminishes over time, reinforcing the practicality of our de-

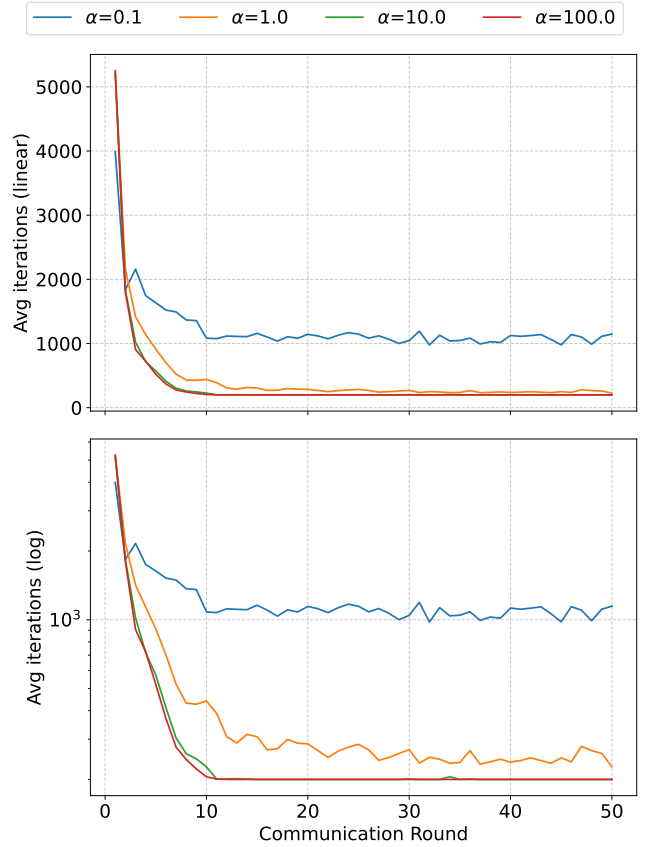


Figure 5: Evolution of GAN training iterations per communication round for different Dirichlet α values on the CIFAR-10 dataset (first 50 rounds shown for clarity). The top subplot (linear scale) highlights absolute iteration trends, while the bottom subplot (log scale) emphasizes relative changes over rounds. Each line shows how the number of iterations required for the generator to converge decreases as FL training progresses. Smaller α values (higher non-IID heterogeneity) require more iterations initially and decline more gradually, whereas larger α (IID) settings converge faster.

fense in long-horizon FL.

6.7 Summary of Results

In summary, our experiments demonstrate that across datasets, attack types, heterogeneity levels, and adversarial proportions, the proposed GAN-based defenses consistently maintain high test accuracy (ACC) while achieving strong detection performance (TPR/TNR). In contrast, baseline methods are brittle, effective only under narrow conditions and prone to collapse under adversarial pressure. Our framework delivers robustness in both benign and adversarial scenarios, making it broadly applicable to real-world federated learning deployments.

7 Limitations and Future Work

While our study demonstrates the effectiveness of the proposed defense framework against generic poisoning attacks, it does not cover all forms of adversarial behavior. Notably, we do not investigate *targeted attacks*, such as backdoor or trigger-based poisoning, where the adversary’s goal is to embed specific malicious behaviors that remain dormant until activated. These attacks can evade detection by maintaining high accuracy on benign data while introducing subtle but harmful effects.

Our evaluation also assumes synchronous training rounds and reliable client participation. Real-world federated learning deployments often involve asynchronous updates and resource-constrained clients, which could affect the applicability of the defense.

Future work includes extending the framework to counter targeted attacks, incorporating backdoor-resilient mechanisms such as trigger detection or adversarial example analysis, and evaluating performance against adaptive adversaries. We also aim to explore large-scale, heterogeneous, and real-world deployments to test practical robustness. Additionally, investigating advanced conditional GAN architectures, such as ccGAN, could improve the quality of synthetic validation data, though at the cost of increased computational resources.

8 Conclusion

In this work, we proposed a GAN-based defense framework for robust federated learning against poisoning attacks. By leveraging a synthetic validation dataset generated via a conditional GAN, our approach effectively identifies and filters malicious client updates while preserving benign contributions. Extensive experiments across MNIST, Fashion-MNIST, and CIFAR-10 demonstrate that our adaptive and clustering-based filtering strategies consistently outperform conventional Byzantine-resilient aggregation methods such as **MULTIKRUM**, achieving higher True Positive Rates in detecting malicious updates and maintaining strong model accuracy in IID and non-IID scenarios. Our analysis also highlights the practical benefits of adaptive filtering: it requires minimal prior knowledge of the dataset and adapts to different data distributions, whereas fixed-threshold approaches struggle to generalize across heterogeneous datasets. Overall, the proposed framework provides a flexible, scalable, and effective defense mechanism for federated learning, offering both strong robustness to a wide range of poisoning strategies and practical applicability in realistic deployment scenarios.

Acknowledgments

The distributed experiments in this work were enabled by access to high-performance computing resources provided

by a national academic supercomputing infrastructure. Additionally, the authors acknowledge the use of an AI language models (DeepSeek-V3 and ChatGPT 4.0) for assistance in refining the manuscript, including improving clarity, structure, and language. The final content and intellectual contributions remain the sole responsibility of the authors.

Ethical Considerations

This work studies poisoning attacks and defenses in federated learning (FL). While developing attack strategies such as label flipping and inner-product manipulation is necessary to evaluate the robustness of defenses, it raises ethical concerns since these methods could, in principle, be misused by adversaries. To mitigate this risk, all experiments are restricted to standard benchmark datasets (e.g., MNIST, CIFAR-10) that do not involve personal or sensitive information, and the contributions are framed primarily around defense evaluation.

In line with responsible disclosure and reproducibility practices, we do not release source code during the anonymous review process. A full release will be made publicly available upon acceptance, ensuring that dissemination occurs within the proper scientific context and supports constructive use.

The value of this work lies in exposing vulnerabilities to strengthen the security and trustworthiness of FL deployments, not in enabling misuse. Consistent with the USENIX ethics policy, we commit to transparency of limitations, careful contextualization of our results, and responsible dissemination to minimize potential harms while advancing defenses for the broader community.

Open Science

In line with the USENIX Security Open Science Policy, we commit to making all research artifacts from this work openly available upon acceptance. These will include the complete source code for model definitions, training pipelines, attack and defense implementations, as well as parameter configurations and experimental logs.

To preserve anonymity during the review process, we do not provide artifact access at this stage. Upon acceptance, however, we will release a permanent DOI-linked repository to ensure long-term availability and reproducibility. Since our experiments rely exclusively on public benchmark datasets and do not involve proprietary or sensitive data, there are no restrictions on artifact sharing.

By releasing all code and data after acceptance, we aim to maximize transparency, reproducibility, and research utility for the security and machine learning communities, while balancing responsible disclosure with the requirements of anonymous review.

References

[1] Youssef Allouah, Sadegh Farhakhani, Rachid Guerraoui, Nirupam Gupta, Rafael Pinot, and John Stephan. Fixing by Mixing: A Recipe for Optimal Byzantine ML under Heterogeneity.

[2] Eugene Bagdasaryan, Andreas Veit, Yiqing Hua, Deborah Estrin, and Vitaly Shmatikov. How To Backdoor Federated Learning.

[3] Peva Blanchard, El Mahdi El Mhamdi, Rachid Guerraoui, and Julien Stainer. Machine Learning with Adversaries: Byzantine Tolerant Gradient Descent. In *Advances in Neural Information Processing Systems*, volume 30. Curran Associates, Inc., 2017.

[4] Carole Cadwalladr. The cambridge analytica files. *The Guardian*, 2018.

[5] Xiaoyu Cao, Minghong Fang, Jia Liu, and Neil Zhenqiang Gong. FLTrust: Byzantine-robust Federated Learning via Trust Bootstrapping, April 2022. arXiv:2012.13995 [cs].

[6] Xiaoyu Cao and Neil Zhenqiang Gong. MPAF: Model Poisoning Attacks to Federated Learning based on Fake Clients, May 2022. arXiv:2203.08669 [cs].

[7] Xinyun Chen, Chang Liu, Bo Li, Kimberly Lu, and Dawn Song. Targeted Backdoor Attacks on Deep Learning Systems Using Data Poisoning, December 2017. arXiv:1712.05526 [cs].

[8] Yudong Chen, Lili Su, and Jiaming Xu. Distributed Statistical Machine Learning in Adversarial Settings: Byzantine Gradient Descent. *Proceedings of the ACM on Measurement and Analysis of Computing Systems*, 1(2):1–25, December 2017.

[9] Federal Trade Commission. Equifax data breach, 2017.

[10] Li Deng. The mnist database of handwritten digit images for machine learning research [best of the web]. *IEEE Signal Processing Magazine*, 29(6):141–142, 2012.

[11] Xin Ding, Yongwei Wang, Zuheng Xu, William J. Welch, and Z. Jane Wang. CcGAN: Continuous Conditional Generative Adversarial Networks for Image Generation.

[12] Minghong Fang, Xiaoyu Cao, Jinyuan Jia, and Neil Gong. Local Model Poisoning Attacks to Byzantine-Robust Federated Learning.

[13] Minghong Fang, Xiaoyu Cao, Jinyuan Jia, and Neil Zhenqiang Gong. Local model poisoning attacks to byzantine-robust federated learning. In *Proceedings of the 29th USENIX Conference on Security Symposium*, SEC’20, pages 1623–1640, USA, August 2020. USENIX Association.

[14] Clement Fung, Chris J. M. Yoon, and Ivan Beschastnikh. The Limitations of Federated Learning in Sybil Settings. In *23rd International Symposium on Research in Attacks, Intrusions and Defenses (RAID 2020)*, pages 301–316, 2020.

[15] Kaiming He, Xiangyu Zhang, Shaoqing Ren, and Jian Sun. Deep residual learning for image recognition. *CoRR*, abs/1512.03385, 2015.

[16] California Legislative Information. California consumer privacy act (ccpa), 2018.

[17] Sai Praneeth Karimireddy, Lie He, and Martin Jaggi. Byzantine-Robust Learning on Heterogeneous Datasets via Bucketing.

[18] Sai Praneeth Karimireddy, Lie He, and Martin Jaggi. Learning from History for Byzantine Robust Optimization.

[19] Sai Praneeth Karimireddy, Lie He, and Martin Jaggi. Learning from History for Byzantine Robust Optimization, June 2021. arXiv:2012.10333 [cs, math, stat].

[20] Alex Krizhevsky and Geoffrey Hinton. Learning multiple layers of features from tiny images. Technical Report 0, University of Toronto, Toronto, Ontario, 2009.

[21] Y. LeCun, L. Bottou, Y. Bengio, and P. Haffner. Gradient-based learning applied to document recognition. *Proceedings of the IEEE*, 86(11):2278–2324, 1998.

[22] Shenghui Li, Edith C.-H. Ngai, and Thimo Voigt. An Experimental Study of Byzantine-Robust Aggregation Schemes in Federated Learning. *IEEE Transactions on Big Data*, pages 1–13, 2023.

[23] Suyi Li, Yong Cheng, Wei Wang, Yang Liu, and Tianjian Chen. Learning to Detect Malicious Clients for Robust Federated Learning, February 2020. arXiv:2002.00211 [cs].

[24] H. Brendan McMahan, Eider Moore, Daniel Ramage, Seth Hampson, and Blaise Agüera y Arcas. Communication-Efficient Learning of Deep Networks from Decentralized Data, January 2023. arXiv:1602.05629 [cs].

[25] El Mahdi El Mhamdi, Rachid Guerraoui, and Sébastien Rouault. The Hidden Vulnerability of Distributed Learning in Byzantium, July 2018. arXiv:1802.07927 [cs, stat].

[26] Mehdi Mirza and Simon Osindero. Conditional generative adversarial nets. *CoRR*, abs/1411.1784, 2014.

[27] Xutong Mu, Ke Cheng, Yulong Shen, Xiaoxiao Li, Zhao Chang, Tao Zhang, and Xindi Ma. FedDMC: Efficient and Robust Federated Learning via Detecting Malicious Clients. *IEEE Transactions on Dependable and Secure Computing*, 21(6):5259–5274, November 2024.

[28] Thien Duc Nguyen, Phillip Rieger, Huili Chen, Hossein Yalame, Helen Möllering, Hossein Fereidooni, Samuel Marchal, Markus Miettinen, Azalia Mirhoseini, Shaza Zeitouni, Farinaz Koushanfar, Ahmad-Reza Sadeghi, and Thomas Schneider. {FLAME}: Taming Backdoors in Federated Learning. In *31st USENIX Security Symposium (USENIX Security 22)*, pages 1415–1432, 2022.

[29] Thien Duc Nguyen, Phillip Rieger, Huili Chen, Hossein Yalame, Helen Möllering, Hossein Fereidooni, Samuel Marchal, Markus Miettinen, Azalia Mirhoseini, Shaza Zeitouni, Farinaz Koushanfar, Ahmad-Reza Sadeghi, and Thomas Schneider. FLAME: Taming Backdoors in Federated Learning (Extended Version 1), August 2023. arXiv:2101.02281 [cs].

[30] Krishna Pillutla, Sham M. Kakade, and Zaid Harchaoui. Robust Aggregation for Federated Learning. *IEEE Transactions on Signal Processing*, 70:1142–1154, 2022.

[31] Phillip Rieger, Thien Duc Nguyen, Markus Miettinen, and Ahmad-Reza Sadeghi. DeepSight: Mitigating Backdoor Attacks in Federated Learning Through Deep Model Inspection. In *Proceedings 2022 Network and Distributed System Security Symposium*, 2022. arXiv:2201.00763 [cs].

[32] Virat Shejwalkar, Amir Houmansadr, Peter Kairouz, and Daniel Ramage. Back to the Drawing Board: A Critical Evaluation of Poisoning Attacks on Production Federated Learning, December 2021. arXiv:2108.10241 [cs].

[33] Shiqi Shen, Shruti Tople, and Prateek Saxena. Auror: Defending against poisoning attacks in collaborative deep learning systems. In *Proceedings of the 32nd Annual Conference on Computer Security Applications*, pages 508–519, Los Angeles California USA, December 2016. ACM.

[34] Gan Sun, Yang Cong, Jiahua Dong, Qiang Wang, and Ji Liu. Data Poisoning Attacks on Federated Machine Learning, April 2020. arXiv:2004.10020 [cs].

[35] Paul Voigt and Axel von dem Bussche. *Material Requirements*, pages 87–140. Springer International Publishing, Cham, 2017.

[36] Han Xiao, Kashif Rasul, and Roland Vollgraf. Fashion-mnist: a novel image dataset for benchmarking machine learning algorithms, 2017.

[37] Qiang Yang, Yang Liu, Tianjian Chen, and Yongxin Tong. Federated Machine Learning: Concept and Applications, February 2019. arXiv:1902.04885 [cs].

[38] Dong Yin, Yudong Chen, Kannan Ramchandran, and Peter Bartlett. Byzantine-Robust Distributed Learning: Towards Optimal Statistical Rates, February 2021. arXiv:1803.01498 [cs, stat].

[39] Kaiyuan Zhang, Guanhong Tao, Qiuling Xu, Siyuan Cheng, Shengwei An, Yingqi Liu, Shiwei Feng, Guangyu Shen, Pin-Yu Chen, Shiqing Ma, and Xiangyu Zhang. FLIP: A Provable Defense Framework for Backdoor Mitigation in Federated Learning, February 2023. arXiv:2210.12873 [cs].

[40] Zaixi Zhang, Xiaoyu Cao, Jinyuan Jia, and Neil Zhen-qiang Gong. FLDetector: Defending Federated Learning Against Model Poisoning Attacks via Detecting Malicious Clients, October 2022. arXiv:2207.09209 [cs].

[41] Ying Zhao, Junjun Chen, Jiale Zhang, Di Wu, Michael Blumenstein, and Shui Yu. Detecting and mitigating poisoning attacks in federated learning using generative adversarial networks. *Concurrency and Computation: Practice and Experience*, 34(7):e5906, March 2022.

A Detailed Experimental Setup

A.1 Training Hyperparameters

All clients use SGD with Nesterov momentum (0.9) and weight decay 1×10^{-4} . The learning rate is fixed at 0.01. Benign clients train for $E = 10$ local epochs with batch size $B = 128$. Malicious-client training specifics are attack-dependent (below).

A.2 Attack Details

We evaluate the robustness of our framework against four types of poisoning attacks: Random Noise, Sign Flipping, Label Flipping, and Backdoor attacks. Below, we provide details on the implementation of each attack:

A.2.1 Random Noise (RN) Attack

Before sending updates, each malicious client perturbs its local model/gradient by additive Gaussian noise:

$$\Delta w \leftarrow \Delta w + \epsilon, \quad \epsilon \sim \mathcal{N}(0, 0.5^2 I).$$

To maximize impact, attackers perform collusion and submit the same perturbed update (sybil-style).

A.2.2 Sign Flipping (SF) Attack

This attack destabilizes the global model by reversing and scaling the direction of gradient updates. Malicious clients reverse and scale their updates to push the global step in the wrong direction. Specifically, each malicious clients submit the following:

$$\Delta w' = -\gamma \Delta w, \quad \text{with } \gamma = 5.0.$$

A.2.3 Label Flipping (LF) Attack

During local training, malicious clients flip the labels of a subset of training samples (e.g., changing label 0 to 9 in MNIST). This attack aims to degrade the global model’s accuracy by introducing incorrect label information. In our experiments, we rotate all labels (e.g., 0 \rightarrow 1, 1 \rightarrow 2, and so on). To amplify impact, malicious clients also scale their submitted updates by a factor of $\gamma = 4.0$.

A.2.4 Inner Product Manipulation (IPM) Attack

The core idea of the IPM attack is to push the aggregated model update in a direction that is *negatively aligned* with the average benign update, thereby obstructing descent of the training loss. Consider a training round t with n total clients, among which m are adversarial and $n - m$ are honest. Denote

the local update of client i as w_t^i , and let the average update of the honest group be

$$\bar{w}_t^{\mathcal{H}} = \frac{1}{n-m} \sum_{i \in \mathcal{H}_t} w_t^i.$$

A canonical IPM construction lets each adversarial client submit a scaled negative copy of this benign mean:

$$w_t^j = -\gamma \bar{w}_t^{\mathcal{H}}, \quad \forall j \in \mathcal{B}_t \quad (2)$$

where $\gamma > 0$ is a tunable attack parameter that determines how aggressively the adversary amplifies the opposition. In practice, the exact value of γ that guarantees maximal disruption is unknown. To address this, each malicious client performs a one-dimensional line search over γ . The idea is to probe multiple candidate scalings of the form

$$w_t^j(\gamma) = -\gamma \tilde{w}_t,$$

where \tilde{w}_t is the adversary’s estimate of the benign mean (e.g., obtained from its own local update or a running historical approximation). For each candidate γ , the adversary evaluates a surrogate loss on its proxy dataset and selects the value of γ that maximizes the inner product

$$\langle w_t^j(\gamma), \tilde{w}_t \rangle,$$

thereby ensuring strongest opposition to the benign direction.

B Additional Results

In this appendix, we provide comprehensive detection results of our framework across all datasets, malicious ratios, attack types, and data heterogeneity levels (Dirichlet α values). To avoid overwhelming the main body, only one representative set of results is presented there (e.g., CIFAR-10, $\alpha = 1.0$), while the full suite is summarized here.

Tables 4–11 report the True Positive Rate (TPR) and True Negative Rate (TNR) for all combinations of datasets (MNIST, Fashion-MNIST, CIFAR-10), fractions of malicious clients (0%, 10%, 20%, 30%), and evaluated defense methods under four attack types (Random Noise, Sign-Flipping, Label-Flipping, Inner Product Manipulation). Each Dirichlet $\alpha \in \{100.0, 10.0, 1.0, 0.1\}$ corresponds to a separate table pair (TPR and TNR), capturing both IID and non-IID regimes.

These tables highlight several key patterns:

- Our adaptive-threshold and clustering-based GAN variants consistently achieve high TPR across datasets and attack types, demonstrating strong detection of malicious updates.
- Benign contributions are preserved effectively, reflected in consistently high TNR values across all scenarios.

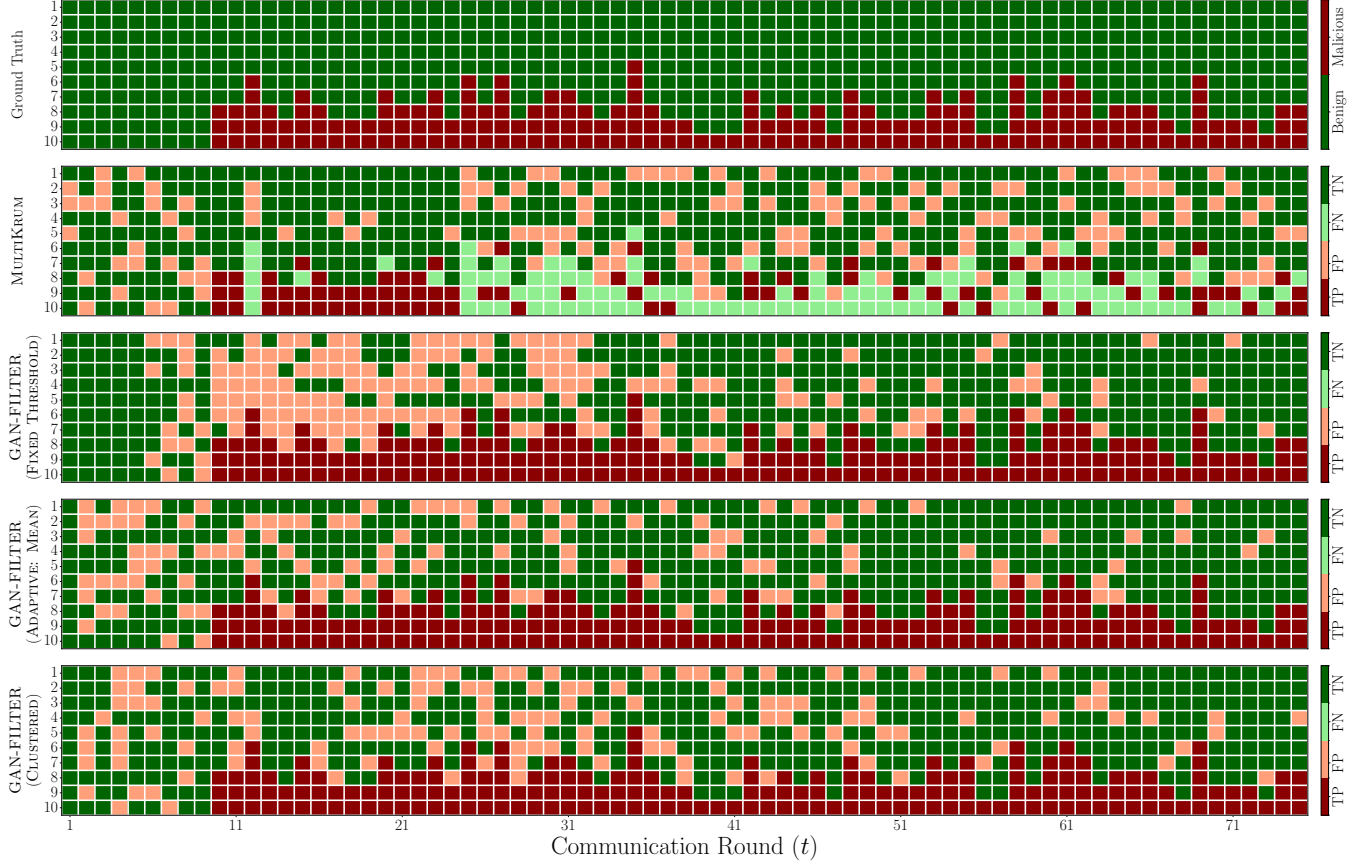


Figure 6: Heatmap comparing MULTIKRUM and proposed method variants under a Random Noise attack under a Random Noise attack with 30% malicious clients on the Fashion-MNIST dataset.

Table 6: True Positive Rate (TPR) of all evaluated defense methods across datasets and malicious client ratios, shown for Dirichlet $\alpha = 10$. Higher values indicate stronger detection of malicious updates.

| Baseline | No Attack | $\epsilon = 10\%$ | | | | $\epsilon = 20\%$ | | | | $\epsilon = 30\%$ | | | | |
|----------|-----------------------|-------------------|------|------|------|-------------------|------|------|------|-------------------|------|------|------|------|
| | | RN | LF | SF | IPM | RN | LF | SF | IPM | RN | LF | SF | IPM | |
| MNIST | MULTIKRUM | 0.00 | 0.68 | 0.67 | 0.54 | 0.61 | 0.64 | 0.68 | 0.68 | 0.39 | 0.33 | 0.63 | 0.77 | 0.30 |
| | GAN (FIXED THRESHOLD) | 0.00 | 1.00 | 1.00 | 1.00 | 1.00 | 1.00 | 1.00 | 1.00 | 1.00 | 1.00 | 1.00 | 1.00 | 1.00 |
| | GAN (ADAPTIVE: MEAN) | 0.00 | 1.00 | 1.00 | 1.00 | 1.00 | 1.00 | 1.00 | 1.00 | 1.00 | 1.00 | 1.00 | 1.00 | 1.00 |
| | GAN (CLUSTERED) | 0.00 | 1.00 | 1.00 | 1.00 | 1.00 | 1.00 | 1.00 | 1.00 | 1.00 | 1.00 | 1.00 | 1.00 | 1.00 |
| FMNIST | MULTIKRUM | 0.00 | 0.68 | 0.67 | 0.49 | 0.56 | 0.73 | 0.73 | 0.59 | 0.30 | 0.34 | 0.59 | 0.72 | 0.29 |
| | GAN (FIXED THRESHOLD) | 0.00 | 1.00 | 1.00 | 1.00 | 1.00 | 1.00 | 1.00 | 1.00 | 1.00 | 1.00 | 1.00 | 1.00 | 1.00 |
| | GAN (ADAPTIVE: MEAN) | 0.00 | 1.00 | 1.00 | 1.00 | 1.00 | 1.00 | 1.00 | 1.00 | 1.00 | 1.00 | 1.00 | 1.00 | 1.00 |
| | GAN (CLUSTERED) | 0.00 | 1.00 | 1.00 | 1.00 | 1.00 | 1.00 | 1.00 | 1.00 | 1.00 | 1.00 | 1.00 | 1.00 | 1.00 |
| CIFAR-10 | MULTIKRUM | 0.00 | 0.68 | 0.68 | 0.68 | 0.57 | 0.73 | 0.75 | 0.76 | 0.70 | 0.70 | 0.77 | 0.83 | 0.54 |
| | GAN (FIXED THRESHOLD) | 0.00 | 1.00 | 1.00 | 1.00 | 1.00 | 1.00 | 1.00 | 1.00 | 1.00 | 1.00 | 1.00 | 1.00 | 1.00 |
| | GAN (ADAPTIVE: MEAN) | 0.00 | 1.00 | 1.00 | 1.00 | 1.00 | 1.00 | 1.00 | 1.00 | 1.00 | 1.00 | 1.00 | 1.00 | 1.00 |
| | GAN (CLUSTERED) | 0.00 | 1.00 | 1.00 | 1.00 | 1.00 | 1.00 | 1.00 | 1.00 | 1.00 | 1.00 | 1.00 | 0.99 | 1.00 |

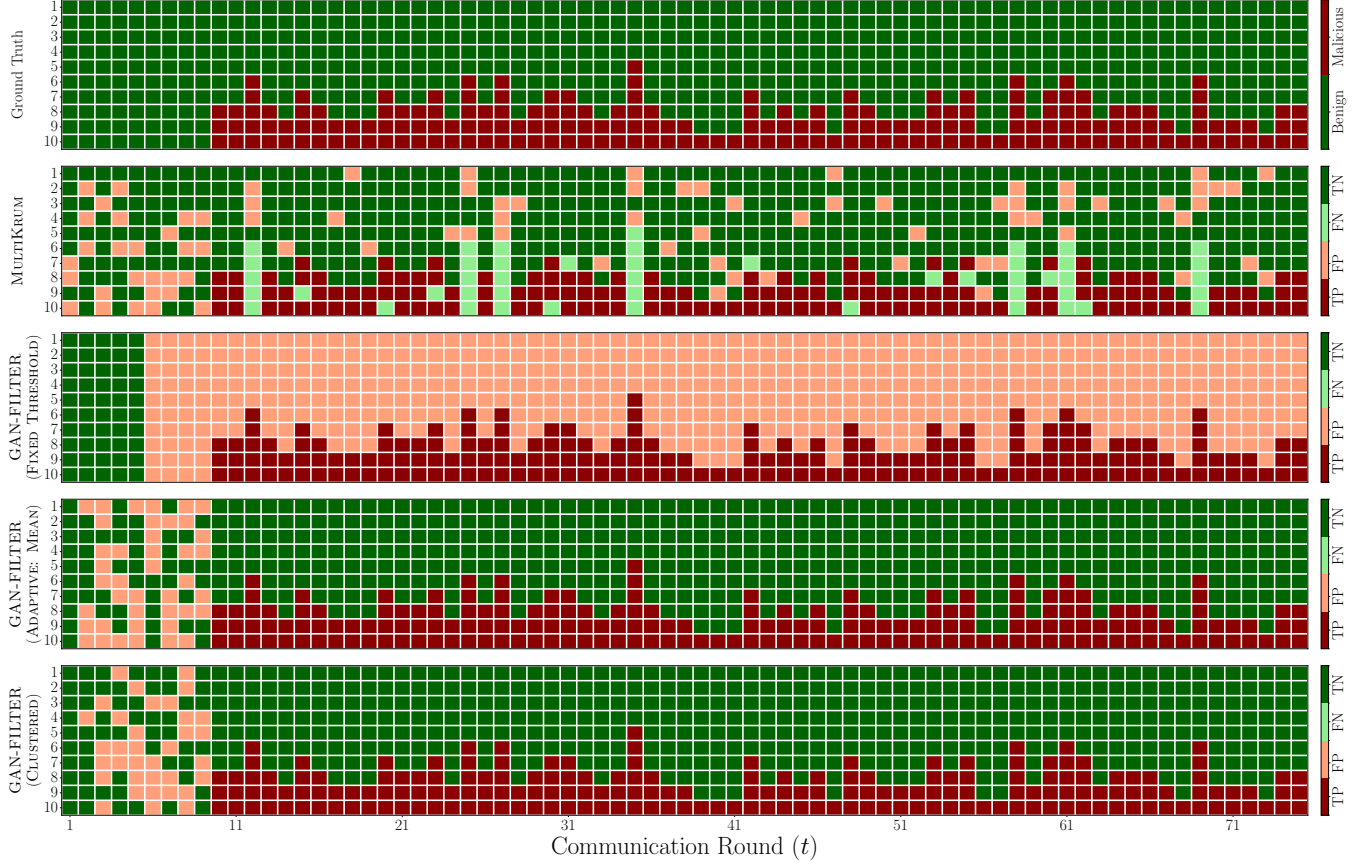


Figure 7: Heatmap showing MULTIKRUM and proposed method performance under a Random Noise attack (30% malicious clients) on the CIFAR-10 dataset. The proposed framework demonstrates robust detection capabilities, outperforming MULTIKRUM in complex settings.

Table 7: True Negative Rate (TNR) of all evaluated defense methods across datasets and malicious client ratios, shown for Dirichlet $\alpha = 10$. Higher values indicate better preservation of benign updates.

| Baseline | No Attack | $\epsilon = 10\%$ | | | | $\epsilon = 20\%$ | | | | $\epsilon = 30\%$ | | | | |
|----------|-----------------------|-------------------|------|------|------|-------------------|------|------|------|-------------------|------|------|------|------|
| | | RN | LF | SF | IPM | RN | LF | SF | IPM | RN | LF | SF | IPM | |
| MNIST | MULTIKRUM | 1.00 | 0.96 | 0.96 | 0.94 | 0.95 | 0.90 | 0.91 | 0.91 | 0.85 | 0.71 | 0.83 | 0.89 | 0.70 |
| | GAN (FIXED THRESHOLD) | 0.99 | 0.99 | 0.99 | 0.98 | 1.00 | 0.98 | 1.00 | 0.99 | 1.00 | 0.99 | 0.98 | 1.00 | 0.98 |
| | GAN (ADAPTIVE: MEAN) | 0.80 | 0.91 | 0.91 | 0.91 | 0.91 | 0.95 | 0.95 | 0.95 | 0.96 | 0.98 | 0.98 | 0.98 | 0.98 |
| | GAN (CLUSTERED) | 0.86 | 0.94 | 0.93 | 0.94 | 0.94 | 0.97 | 0.97 | 0.97 | 0.97 | 0.98 | 0.98 | 0.98 | 0.98 |
| FMNIST | MULTIKRUM | 1.00 | 0.96 | 0.96 | 0.94 | 0.95 | 0.92 | 0.92 | 0.89 | 0.82 | 0.72 | 0.82 | 0.87 | 0.69 |
| | GAN (FIXED THRESHOLD) | 0.76 | 0.81 | 0.81 | 0.79 | 0.60 | 0.63 | 0.79 | 0.77 | 0.72 | 0.67 | 0.79 | 0.77 | 0.79 |
| | GAN (ADAPTIVE: MEAN) | 0.72 | 0.79 | 0.78 | 0.76 | 0.76 | 0.81 | 0.80 | 0.80 | 0.82 | 0.82 | 0.81 | 0.81 | 0.84 |
| | GAN (CLUSTERED) | 0.78 | 0.82 | 0.83 | 0.81 | 0.81 | 0.85 | 0.82 | 0.84 | 0.83 | 0.87 | 0.86 | 0.87 | 0.85 |
| CIFAR-10 | MULTIKRUM | 1.00 | 0.96 | 0.96 | 0.96 | 0.95 | 0.92 | 0.93 | 0.93 | 0.92 | 0.86 | 0.89 | 0.91 | 0.79 |
| | GAN (FIXED THRESHOLD) | 0.03 | 0.03 | 0.03 | 0.03 | 0.03 | 0.03 | 0.03 | 0.03 | 0.03 | 0.03 | 0.03 | 0.03 | 0.03 |
| | GAN (ADAPTIVE: MEAN) | 0.59 | 0.83 | 0.83 | 0.83 | 0.83 | 0.92 | 0.91 | 0.92 | 0.92 | 0.96 | 0.96 | 0.96 | 0.96 |
| | GAN (CLUSTERED) | 0.68 | 0.86 | 0.85 | 0.85 | 0.86 | 0.93 | 0.93 | 0.93 | 0.93 | 0.96 | 0.96 | 0.97 | 0.96 |

Table 8: True Positive Rate (TPR) of all evaluated defense methods across datasets and malicious client ratios, shown for Dirichlet $\alpha = 1.0$. Higher values indicate stronger detection of malicious updates.

| Baseline | No Attack | $\epsilon = 10\%$ | | | | $\epsilon = 20\%$ | | | | $\epsilon = 30\%$ | | | | |
|----------|-----------------------|-------------------|------|------|------|-------------------|------|------|------|-------------------|------|------|------|------|
| | | RN | LF | SF | IPM | RN | LF | SF | IPM | RN | LF | SF | IPM | |
| MNIST | MULTIKRUM | 0.00 | 0.68 | 0.67 | 0.67 | 0.62 | 0.60 | 0.74 | 0.68 | 0.33 | 0.34 | 0.60 | 0.72 | 0.29 |
| | GAN (FIXED THRESHOLD) | 0.00 | 1.00 | 1.00 | 1.00 | 1.00 | 1.00 | 1.00 | 1.00 | 1.00 | 1.00 | 1.00 | 1.00 | 1.00 |
| | GAN (ADAPTIVE: MEAN) | 0.00 | 1.00 | 1.00 | 1.00 | 1.00 | 1.00 | 1.00 | 1.00 | 1.00 | 1.00 | 1.00 | 1.00 | 1.00 |
| | GAN (CLUSTERED) | 0.00 | 1.00 | 1.00 | 1.00 | 1.00 | 1.00 | 1.00 | 1.00 | 1.00 | 1.00 | 1.00 | 1.00 | 1.00 |
| FMNIST | MULTIKRUM | 0.00 | 0.68 | 0.67 | 0.63 | 0.60 | 0.71 | 0.74 | 0.56 | 0.32 | 0.32 | 0.66 | 0.64 | 0.30 |
| | GAN (FIXED THRESHOLD) | 0.00 | 1.00 | 1.00 | 1.00 | 1.00 | 1.00 | 1.00 | 1.00 | 1.00 | 1.00 | 1.00 | 1.00 | 1.00 |
| | GAN (ADAPTIVE: MEAN) | 0.00 | 1.00 | 1.00 | 1.00 | 1.00 | 1.00 | 1.00 | 1.00 | 1.00 | 1.00 | 1.00 | 1.00 | 1.00 |
| | GAN (CLUSTERED) | 0.00 | 1.00 | 1.00 | 1.00 | 1.00 | 1.00 | 0.95 | 1.00 | 1.00 | 1.00 | 0.94 | 1.00 | 1.00 |
| CIFAR-10 | MULTIKRUM | 0.00 | 0.68 | 0.68 | 0.68 | 0.65 | 0.73 | 0.75 | 0.76 | 0.72 | 0.70 | 0.82 | 0.83 | 0.49 |
| | GAN (FIXED THRESHOLD) | 0.00 | 1.00 | 1.00 | 1.00 | 1.00 | 1.00 | 1.00 | 1.00 | 1.00 | 1.00 | 1.00 | 1.00 | 1.00 |
| | GAN (ADAPTIVE: MEAN) | 0.00 | 1.00 | 1.00 | 1.00 | 1.00 | 1.00 | 0.99 | 1.00 | 1.00 | 1.00 | 0.98 | 0.98 | 1.00 |
| | GAN (CLUSTERED) | 0.00 | 1.00 | 0.96 | 0.97 | 1.00 | 1.00 | 0.96 | 0.94 | 1.00 | 1.00 | 0.94 | 0.86 | 1.00 |

Table 9: True Negative Rate (TNR) of all evaluated defense methods across datasets and malicious client ratios, shown for Dirichlet $\alpha = 1.0$. Higher values indicate better preservation of benign updates.

| Baseline | No Attack | $\epsilon = 10\%$ | | | | $\epsilon = 20\%$ | | | | $\epsilon = 30\%$ | | | | |
|----------|-----------------------|-------------------|------|------|------|-------------------|------|------|------|-------------------|------|------|------|------|
| | | RN | LF | SF | IPM | RN | LF | SF | IPM | RN | LF | SF | IPM | |
| MNIST | MULTIKRUM | 1.00 | 0.96 | 0.96 | 0.96 | 0.95 | 0.89 | 0.92 | 0.91 | 0.83 | 0.71 | 0.82 | 0.86 | 0.70 |
| | GAN (FIXED THRESHOLD) | 0.98 | 0.98 | 0.98 | 0.98 | 0.98 | 0.98 | 0.98 | 0.98 | 0.98 | 0.98 | 0.98 | 0.97 | 0.98 |
| | GAN (ADAPTIVE: MEAN) | 0.83 | 0.91 | 0.91 | 0.91 | 0.92 | 0.95 | 0.95 | 0.95 | 0.95 | 0.97 | 0.97 | 0.97 | 0.97 |
| | GAN (CLUSTERED) | 0.86 | 0.93 | 0.94 | 0.93 | 0.94 | 0.96 | 0.96 | 0.96 | 0.96 | 0.98 | 0.97 | 0.97 | 0.98 |
| FMNIST | MULTIKRUM | 1.00 | 0.96 | 0.96 | 0.95 | 0.95 | 0.92 | 0.93 | 0.88 | 0.83 | 0.71 | 0.84 | 0.84 | 0.70 |
| | GAN (FIXED THRESHOLD) | 0.11 | 0.15 | 0.27 | 0.15 | 0.11 | 0.31 | 0.44 | 0.36 | 0.23 | 0.19 | 0.13 | 0.33 | 0.27 |
| | GAN (ADAPTIVE: MEAN) | 0.62 | 0.64 | 0.64 | 0.66 | 0.64 | 0.70 | 0.69 | 0.69 | 0.68 | 0.73 | 0.74 | 0.72 | 0.73 |
| | GAN (CLUSTERED) | 0.65 | 0.67 | 0.69 | 0.70 | 0.66 | 0.69 | 0.78 | 0.71 | 0.68 | 0.70 | 0.73 | 0.70 | 0.72 |
| CIFAR-10 | MULTIKRUM | 1.00 | 0.96 | 0.96 | 0.96 | 0.96 | 0.92 | 0.93 | 0.93 | 0.92 | 0.86 | 0.90 | 0.91 | 0.78 |
| | GAN (FIXED THRESHOLD) | 0.03 | 0.03 | 0.03 | 0.03 | 0.03 | 0.03 | 0.03 | 0.03 | 0.03 | 0.03 | 0.03 | 0.03 | 0.03 |
| | GAN (ADAPTIVE: MEAN) | 0.57 | 0.83 | 0.76 | 0.81 | 0.83 | 0.92 | 0.86 | 0.90 | 0.92 | 0.96 | 0.92 | 0.95 | 0.96 |
| | GAN (CLUSTERED) | 0.66 | 0.86 | 0.85 | 0.86 | 0.87 | 0.94 | 0.93 | 0.94 | 0.93 | 0.97 | 0.96 | 0.97 | 0.96 |

- The impact of data heterogeneity is visible: as α decreases (more non-IID), TPR/TNR can slightly vary, emphasizing the importance of adaptive defenses.
- Comparisons with baseline aggregation schemes such as MULTIKRUM, MEDIAN, and TRIMAVG reveal substantial improvements in adversarial resilience, especially under high malicious client ratios.

Table 10: True Positive Rate (TPR) of all evaluated defense methods across datasets and malicious client ratios, shown for Dirichlet $\alpha = 0.1$. Higher values indicate stronger detection of malicious updates.

| Baseline | No Attack | $\epsilon = 10\%$ | | | | $\epsilon = 20\%$ | | | | $\epsilon = 30\%$ | | | | |
|----------|-----------------------|-------------------|------|------|------|-------------------|------|------|------|-------------------|------|------|------|------|
| | | RN | LF | SF | IPM | RN | LF | SF | IPM | RN | LF | SF | IPM | |
| MNIST | MULTIKRUM | 0.00 | 0.68 | 0.59 | 0.49 | 0.65 | 0.63 | 0.66 | 0.71 | 0.31 | 0.31 | 0.68 | 0.72 | 0.29 |
| | GAN (FIXED THRESHOLD) | 0.00 | 1.00 | 1.00 | 1.00 | 1.00 | 1.00 | 1.00 | 1.00 | 1.00 | 1.00 | 1.00 | 1.00 | 1.00 |
| | GAN (ADAPTIVE: MEAN) | 0.00 | 0.98 | 0.96 | 0.99 | 1.00 | 0.99 | 0.92 | 0.99 | 1.00 | 0.99 | 0.88 | 0.98 | 1.00 |
| | GAN (CLUSTERED) | 0.00 | 0.98 | 0.89 | 0.98 | 1.00 | 0.98 | 0.87 | 0.98 | 1.00 | 0.99 | 0.82 | 0.97 | 1.00 |
| FMNIST | MULTIKRUM | 0.00 | 0.68 | 0.61 | 0.56 | 0.53 | 0.59 | 0.70 | 0.33 | 0.20 | 0.32 | 0.71 | 0.82 | 0.29 |
| | GAN (FIXED THRESHOLD) | 0.00 | 1.00 | 1.00 | 1.00 | 1.00 | 1.00 | 1.00 | 1.00 | 1.00 | 1.00 | 1.00 | 1.00 | 1.00 |
| | GAN (ADAPTIVE: MEAN) | 0.00 | 0.99 | 0.96 | 1.00 | 1.00 | 0.99 | 0.96 | 1.00 | 1.00 | 0.99 | 0.95 | 1.00 | 1.00 |
| | GAN (CLUSTERED) | 0.00 | 0.97 | 0.98 | 0.96 | 1.00 | 0.98 | 0.97 | 0.96 | 1.00 | 0.99 | 0.97 | 0.97 | 1.00 |
| CIFAR-10 | MULTIKRUM | 0.00 | 0.68 | 0.66 | 0.68 | 0.67 | 0.73 | 0.74 | 0.76 | 0.73 | 0.70 | 0.80 | 0.83 | 0.53 |
| | GAN (FIXED THRESHOLD) | 0.00 | 1.00 | 1.00 | 1.00 | 1.00 | 1.00 | 1.00 | 1.00 | 1.00 | 1.00 | 1.00 | 1.00 | 1.00 |
| | GAN (ADAPTIVE: MEAN) | 0.00 | 1.00 | 0.94 | 0.97 | 1.00 | 1.00 | 0.91 | 0.94 | 1.00 | 1.00 | 0.84 | 0.88 | 1.00 |
| | GAN (CLUSTERED) | 0.00 | 1.00 | 0.87 | 0.90 | 1.00 | 1.00 | 0.77 | 0.81 | 1.00 | 1.00 | 0.69 | 0.74 | 1.00 |

Table 11: True Negative Rate (TNR) of all evaluated defense methods across datasets and malicious client ratios, shown for Dirichlet $\alpha = 0.1$. Higher values indicate better preservation of benign updates.

| Baseline | No Attack | $\epsilon = 10\%$ | | | | $\epsilon = 20\%$ | | | | $\epsilon = 30\%$ | | | | |
|----------|-----------------------|-------------------|------|------|------|-------------------|------|------|------|-------------------|------|------|------|------|
| | | RN | LF | SF | IPM | RN | LF | SF | IPM | RN | LF | SF | IPM | |
| MNIST | MULTIKRUM | 1.00 | 0.96 | 0.95 | 0.94 | 0.96 | 0.90 | 0.91 | 0.92 | 0.83 | 0.71 | 0.85 | 0.86 | 0.69 |
| | GAN (FIXED THRESHOLD) | 0.03 | 0.03 | 0.03 | 0.03 | 0.03 | 0.03 | 0.03 | 0.03 | 0.03 | 0.03 | 0.03 | 0.03 | 0.03 |
| | GAN (ADAPTIVE: MEAN) | 0.61 | 0.73 | 0.72 | 0.73 | 0.79 | 0.76 | 0.76 | 0.82 | 0.82 | 0.80 | 0.81 | 0.88 | 0.91 |
| | GAN (CLUSTERED) | 0.73 | 0.78 | 0.81 | 0.82 | 0.84 | 0.70 | 0.81 | 0.89 | 0.90 | 0.89 | 0.86 | 0.94 | 0.95 |
| FMNIST | MULTIKRUM | 1.00 | 0.96 | 0.95 | 0.95 | 0.94 | 0.89 | 0.91 | 0.83 | 0.80 | 0.71 | 0.86 | 0.91 | 0.70 |
| | GAN (FIXED THRESHOLD) | 0.03 | 0.02 | 0.03 | 0.03 | 0.03 | 0.03 | 0.03 | 0.03 | 0.03 | 0.03 | 0.03 | 0.03 | 0.02 |
| | GAN (ADAPTIVE: MEAN) | 0.36 | 0.39 | 0.38 | 0.39 | 0.39 | 0.39 | 0.41 | 0.43 | 0.42 | 0.37 | 0.45 | 0.38 | 0.20 |
| | GAN (CLUSTERED) | 0.26 | 0.63 | 0.28 | 0.39 | 0.28 | 0.68 | 0.29 | 0.55 | 0.56 | 0.73 | 0.32 | 0.58 | 0.97 |
| CIFAR-10 | MULTIKRUM | 1.00 | 0.96 | 0.96 | 0.96 | 0.96 | 0.92 | 0.92 | 0.93 | 0.92 | 0.86 | 0.90 | 0.91 | 0.79 |
| | GAN (FIXED THRESHOLD) | 0.03 | 0.03 | 0.03 | 0.03 | 0.03 | 0.03 | 0.03 | 0.03 | 0.03 | 0.03 | 0.03 | 0.03 | 0.03 |
| | GAN (ADAPTIVE: MEAN) | 0.57 | 0.76 | 0.68 | 0.76 | 0.82 | 0.86 | 0.75 | 0.86 | 0.91 | 0.92 | 0.83 | 0.93 | 0.96 |
| | GAN (CLUSTERED) | 0.64 | 0.84 | 0.78 | 0.84 | 0.84 | 0.92 | 0.84 | 0.92 | 0.93 | 0.96 | 0.91 | 0.96 | 0.97 |

Table 12: Overall test accuracy (ACC) of federated learning under benign training and poisoning attacks across malicious client fractions (10%, 20%, 30%) in the low non-IID setting $\alpha = 10$. Results are reported on MNIST, Fashion-MNIST, and CIFAR-10, comparing standard aggregation rules (FEDAVG, MEDIAN, TRIMMED MEAN, GEOMEDIAN, KRM, NNM+KRM) against our proposed GAN-based authentication variants. GAN-based defenses consistently preserve accuracy even under high adversarial presence, whereas conventional robust aggregation methods degrade significantly.

| Baseline | No Attack | $\epsilon = 10\%$ | | | | $\epsilon = 20\%$ | | | | $\epsilon = 30\%$ | | | |
|---------------|-----------------------|-------------------|------|------|------|-------------------|------|------|------|-------------------|------|------|------|
| | | RN | LF | SF | IPM | RN | LF | SF | IPM | RN | LF | SF | IPM |
| MNIST | FEDAVG | 0.99 | 0.47 | 0.98 | 0.11 | 0.11 | 0.52 | 0.11 | 0.10 | 0.11 | 0.13 | 0.10 | 0.10 |
| | MEDIAN | 0.99 | 0.99 | 0.99 | 0.99 | 0.99 | 0.94 | 0.11 | 0.99 | 0.10 | 0.10 | 0.11 | 0.10 |
| | TRIMAVG | 0.99 | 0.93 | 0.99 | 0.98 | 0.10 | 0.40 | 0.98 | 0.11 | 0.10 | 0.10 | 0.11 | 0.10 |
| | GEOMEDIAN | 0.99 | 0.99 | 0.99 | 0.99 | 0.99 | 0.95 | 0.99 | 0.99 | 0.10 | 0.10 | 0.10 | 0.10 |
| | MULTIKRM | 0.99 | 0.93 | 0.99 | 0.98 | 0.11 | 0.81 | 0.98 | 0.97 | 0.10 | 0.10 | 0.11 | 0.81 |
| | NNM+KRM | 0.99 | 0.92 | 0.99 | 0.98 | 0.10 | 0.89 | 0.11 | 0.11 | 0.10 | 0.10 | 0.11 | 0.10 |
| | GAN (FIXED THRESHOLD) | 0.99 | 0.99 | 0.99 | 0.99 | 0.99 | 0.99 | 0.99 | 0.99 | 0.99 | 0.99 | 0.99 | 0.99 |
| Fashion MNIST | GAN (ADAPTIVE: MEAN) | 0.99 | 0.99 | 0.99 | 0.99 | 0.99 | 0.99 | 0.99 | 0.99 | 0.99 | 0.99 | 0.99 | 0.99 |
| | GAN (CLUSTERED) | 0.99 | 0.99 | 0.99 | 0.99 | 0.99 | 0.99 | 0.99 | 0.99 | 0.99 | 0.99 | 0.99 | 0.99 |
| | FEDAVG | 0.89 | 0.19 | 0.88 | 0.10 | 0.10 | 0.30 | 0.10 | 0.10 | 0.10 | 0.15 | 0.35 | 0.10 |
| | MEDIAN | 0.89 | 0.88 | 0.88 | 0.88 | 0.88 | 0.68 | 0.78 | 0.86 | 0.10 | 0.10 | 0.10 | 0.10 |
| | TRIMAVG | 0.89 | 0.69 | 0.88 | 0.78 | 0.10 | 0.68 | 0.82 | 0.10 | 0.10 | 0.10 | 0.10 | 0.10 |
| | GEOMEDIAN | 0.89 | 0.88 | 0.89 | 0.88 | 0.89 | 0.81 | 0.85 | 0.87 | 0.10 | 0.10 | 0.10 | 0.10 |
| | MULTIKRM | 0.89 | 0.78 | 0.89 | 0.84 | 0.10 | 0.12 | 0.87 | 0.10 | 0.10 | 0.10 | 0.10 | 0.79 |
| CIFAR-10 | NNM+KRM | 0.89 | 0.74 | 0.89 | 0.10 | 0.10 | 0.70 | 0.84 | 0.10 | 0.10 | 0.10 | 0.10 | 0.10 |
| | GAN (FIXED THRESHOLD) | 0.89 | 0.89 | 0.89 | 0.89 | 0.89 | 0.89 | 0.89 | 0.89 | 0.89 | 0.89 | 0.89 | 0.89 |
| | GAN (ADAPTIVE: MEAN) | 0.90 | 0.89 | 0.89 | 0.89 | 0.89 | 0.89 | 0.89 | 0.89 | 0.89 | 0.89 | 0.89 | 0.89 |
| | GAN (CLUSTERED) | 0.89 | 0.89 | 0.89 | 0.89 | 0.89 | 0.89 | 0.89 | 0.89 | 0.89 | 0.89 | 0.88 | 0.89 |
| | FEDAVG | 0.88 | 0.12 | 0.87 | 0.57 | 0.10 | 0.11 | 0.86 | 0.11 | 0.10 | 0.11 | 0.62 | 0.10 |
| | MEDIAN | 0.88 | 0.87 | 0.87 | 0.86 | 0.86 | 0.42 | 0.86 | 0.81 | 0.10 | 0.18 | 0.84 | 0.72 |
| | TRIMAVG | 0.89 | 0.13 | 0.88 | 0.81 | 0.23 | 0.12 | 0.86 | 0.76 | 0.66 | 0.12 | 0.84 | 0.61 |
| CIFAR-10 | GEOMEDIAN | 0.89 | 0.88 | 0.88 | 0.86 | 0.86 | 0.44 | 0.87 | 0.82 | 0.19 | 0.20 | 0.86 | 0.76 |
| | MULTIKRM | 0.88 | 0.13 | 0.88 | 0.82 | 0.10 | 0.12 | 0.87 | 0.80 | 0.10 | 0.12 | 0.85 | 0.73 |
| | NNM+KRM | 0.89 | 0.13 | 0.88 | 0.83 | 0.10 | 0.12 | 0.87 | 0.79 | 0.29 | 0.12 | 0.84 | 0.72 |
| | GAN (FIXED THRESHOLD) | 0.56 | 0.56 | 0.57 | 0.56 | 0.57 | 0.56 | 0.57 | 0.57 | 0.56 | 0.56 | 0.56 | 0.56 |
| | GAN (ADAPTIVE: MEAN) | 0.87 | 0.88 | 0.88 | 0.88 | 0.88 | 0.88 | 0.87 | 0.88 | 0.88 | 0.87 | 0.87 | 0.87 |
| | GAN (CLUSTERED) | 0.88 | 0.88 | 0.88 | 0.88 | 0.88 | 0.88 | 0.87 | 0.87 | 0.88 | 0.87 | 0.87 | 0.87 |

*we set $\beta = 0.1, 0.2, 0.3$ (where β is byzantine aggregation heuristic, for TRIMAVG and MULTIKRM respectively under 10%, 20%, and 30% malicious clients.

Table 13: Overall test accuracy (ACC) of federated learning under benign training and poisoning attacks across malicious client fractions (10%, 20%, 30%) in the moderate non-IID setting $\alpha = 1.0$. Results are reported on MNIST, Fashion-MNIST, and CIFAR-10, comparing standard aggregation rules (FEDAVG, MEDIAN, TRIMMED MEAN, GEOMEDIAN, KRUM, NNM+KRUM) against our proposed GAN-based authentication variants. GAN-based defenses consistently preserve accuracy even under high adversarial presence, whereas conventional robust aggregation methods degrade significantly.

| Baseline | No Attack | $\epsilon = 10\%$ | | | | $\epsilon = 20\%$ | | | | $\epsilon = 30\%$ | | | |
|---------------|-----------------------|-------------------|------|------|------|-------------------|------|------|------|-------------------|------|------|------|
| | | RN | LF | SF | IPM | RN | LF | SF | IPM | RN | LF | SF | IPM |
| MNIST | FEDAVG | 0.99 | 0.88 | 0.99 | 0.11 | 0.10 | 0.62 | 0.96 | 0.10 | 0.11 | 0.10 | 0.11 | 0.10 |
| | MEDIAN | 0.99 | 0.99 | 0.99 | 0.99 | 0.99 | 0.92 | 0.98 | 0.98 | 0.10 | 0.10 | 0.10 | 0.10 |
| | TRIMAVG | 0.99 | 0.87 | 0.99 | 0.98 | 0.10 | 0.81 | 0.98 | 0.10 | 0.10 | 0.10 | 0.11 | 0.10 |
| | GEOMEDIAN | 0.99 | 0.99 | 0.99 | 0.99 | 0.99 | 0.94 | 0.99 | 0.99 | 0.10 | 0.10 | 0.11 | 0.10 |
| | MULTIKRUM | 0.99 | 0.92 | 0.99 | 0.97 | 0.10 | 0.78 | 0.99 | 0.93 | 0.10 | 0.10 | 0.11 | 0.10 |
| | NNM+KRUM | 0.99 | 0.92 | 0.99 | 0.94 | 0.10 | 0.85 | 0.98 | 0.10 | 0.10 | 0.10 | 0.11 | 0.10 |
| | GAN (FIXED THRESHOLD) | 0.99 | 0.99 | 0.99 | 0.99 | 0.99 | 0.99 | 0.99 | 0.99 | 0.99 | 0.99 | 0.99 | 0.99 |
| Fashion MNIST | GAN (ADAPTIVE: MEAN) | 0.99 | 0.99 | 0.99 | 0.99 | 0.99 | 0.99 | 0.99 | 0.99 | 0.99 | 0.99 | 0.99 | 0.99 |
| | GAN (CLUSTERED) | 0.99 | 0.99 | 0.99 | 0.99 | 0.99 | 0.99 | 0.99 | 0.99 | 0.99 | 0.99 | 0.99 | 0.99 |
| | FEDAVG | 0.88 | 0.71 | 0.86 | 0.10 | 0.10 | 0.21 | 0.81 | 0.10 | 0.10 | 0.10 | 0.27 | 0.10 |
| | MEDIAN | 0.88 | 0.88 | 0.87 | 0.87 | 0.88 | 0.67 | 0.85 | 0.85 | 0.10 | 0.10 | 0.10 | 0.10 |
| | TRIMAVG | 0.89 | 0.60 | 0.87 | 0.85 | 0.10 | 0.67 | 0.85 | 0.10 | 0.10 | 0.10 | 0.80 | 0.10 |
| | GEOMEDIAN | 0.88 | 0.88 | 0.88 | 0.88 | 0.88 | 0.79 | 0.86 | 0.86 | 0.10 | 0.10 | 0.10 | 0.10 |
| | MULTIKRUM | 0.89 | 0.74 | 0.88 | 0.10 | 0.10 | 0.64 | 0.87 | 0.77 | 0.10 | 0.10 | 0.10 | 0.10 |
| CIFAR-10 | NNM+KRUM | 0.89 | 0.50 | 0.88 | 0.75 | 0.10 | 0.70 | 0.87 | 0.10 | 0.10 | 0.10 | 0.10 | 0.10 |
| | GAN (FIXED THRESHOLD) | 0.87 | 0.88 | 0.88 | 0.87 | 0.87 | 0.88 | 0.87 | 0.87 | 0.87 | 0.87 | 0.87 | 0.87 |
| | GAN (ADAPTIVE: MEAN) | 0.88 | 0.88 | 0.88 | 0.88 | 0.88 | 0.88 | 0.88 | 0.88 | 0.88 | 0.88 | 0.87 | 0.88 |
| | GAN (CLUSTERED) | 0.89 | 0.88 | 0.88 | 0.88 | 0.88 | 0.88 | 0.88 | 0.88 | 0.88 | 0.88 | 0.88 | 0.88 |
| | FEDAVG | 0.87 | 0.11 | 0.86 | 0.34 | 0.10 | 0.11 | 0.84 | 0.12 | 0.10 | 0.11 | 0.62 | 0.10 |
| | MEDIAN | 0.87 | 0.85 | 0.85 | 0.85 | 0.84 | 0.37 | 0.84 | 0.80 | 0.10 | 0.16 | 0.82 | 0.70 |
| | TRIMAVG | 0.87 | 0.12 | 0.86 | 0.80 | 0.22 | 0.12 | 0.85 | 0.71 | 0.51 | 0.14 | 0.81 | 0.55 |
| CIFAR-10 | GEOMEDIAN | 0.87 | 0.86 | 0.86 | 0.85 | 0.84 | 0.38 | 0.86 | 0.80 | 0.71 | 0.22 | 0.83 | 0.75 |
| | MULTIKRUM | 0.88 | 0.12 | 0.86 | 0.80 | 0.10 | 0.12 | 0.86 | 0.73 | 0.10 | 0.16 | 0.85 | 0.69 |
| | NNM+KRUM | 0.87 | 0.12 | 0.86 | 0.80 | 0.10 | 0.12 | 0.85 | 0.71 | 0.30 | 0.12 | 0.85 | 0.66 |
| | GAN (FIXED THRESHOLD) | 0.51 | 0.53 | 0.52 | 0.51 | 0.53 | 0.53 | 0.52 | 0.53 | 0.51 | 0.53 | 0.51 | 0.52 |
| | GAN (ADAPTIVE: MEAN) | 0.85 | 0.86 | 0.87 | 0.86 | 0.87 | 0.86 | 0.87 | 0.86 | 0.86 | 0.86 | 0.86 | 0.86 |
| | GAN (CLUSTERED) | 0.87 | 0.86 | 0.86 | 0.86 | 0.86 | 0.86 | 0.86 | 0.85 | 0.86 | 0.85 | 0.86 | 0.86 |

*we set $\beta = 0.1, 0.2, 0.3$ (where β is byzantine aggregation heuristic, for TRIMAVG and MULTIKRUM respectively under 10%, 20%, and 30% malicious clients.